SUB | NIEDERSÄCHSISCHE STAATS- UND UNIVERSITÄTSBIBLIOTHEK GÖTTINGEN

Werk

Jahr: 1988
Kollektion: fid.geo
Signatur: 8 Z NAT 2148:62
Digitalisiert: Niedersächsische Staats- und Universitätsbibliothek Göttingen
Werk Id: PPN1015067948_0062
PURL: http://resolver.sub.uni-goettingen.de/purl?PPN1015067948_0062

LOG Id: LOG_0023
LOG Titel: Results of the DEKORP 4/KTB Oberpfalz deep seismic reflection investigations
LOG Typ: article

Übergeordnetes Werk

Werk Id: PPN1015067948
PURL: http://resolver.sub.uni-goettingen.de/purl?PPN1015067948
OPAC: http://opac.sub.uni-goettingen.de/DB=1/PPN?PPN=1015067948

Terms and Conditions

The Goettingen State and University Library provides access to digitized documents strictly for noncommercial educational, research and private purposes and makes no warranty with regard to their use for other purposes. Some of our collections are protected by copyright. Publication and/or broadcast in any form (including electronic) requires prior written permission from the Goettingen State- and University Library.
Each copy of any part of this document must contain there Terms and Conditions. With the usage of the library's online system to access or download a digitized document you accept the Terms and Conditions.
Reproductions of material on the web site may not be made for or donated to other repositories, nor may be further reproduced without written permission from the Goettingen State- and University Library.

For reproduction requests and permissions, please contact us. If citing materials, please give proper attribution of the source.

Contact

Niedersächsische Staats- und Universitätsbibliothek Göttingen
Georg-August-Universität Göttingen
Platz der Göttinger Sieben 1
37073 Göttingen
Germany
Email: gdz@sub.uni-goettingen.de

J Geophys (1988) 62:69–101

Journal of Geophysics

Results of the DEKORP 4/KTB Oberpfalz deep seismic reflection investigations

DEKORP Research Group

Contributors: **R.K. Bortfeld, F. Keller, B. Sieron, W. Söllner, M. Stiller, R. Thomas** (DEKORP Processing Center, Institut für Geophysik, Arnold-Sommerfeld-Str. 1, 3392 Clausthal-Zellerfeld); **W. Franke** (Institut für Geowissenschaften, Senckenbergstr. 3, 6300 Gießen); **K. Weber, A. Vollbrecht, T. Heinrichs** (Institut für Geologie und Dynamik der Lithosphäre, Goldschmidtstr. 3, 3400 Göttingen); **H.-J. Dürbaum, C. Reichert, J. Schmoll** (Bundesanstalt für Geowissenschaften und Rohstoffe/Niedersächsisches Landesamt für Bodenforschung, Stilleweg 2, 3000 Hannover 51); **G. Dohr** (Preussag AG, Arndtstr. 1, 3000 Hannover 1); **R. Meissner, R. Bittner** (Institut für Geophysik, Olshausenstr. 40–60, 2300 Kiel 1); **H. Gebrande, M. Bopp, P. Neurieder, T. Schmidt** (Institut für Allgemeine und Angewandte Geophysik, Theresienstr. 41/IV, 8000 München 2)

Abstract. In the Oberpfalz-Oberfranken area (NE Bavaria) deep seismic reflection investigations were jointly carried out in 1985 for two important geo-scientific programmes: DEKORP and KTB. The network of lines consists of one long DEKORP profile, DEKORP 4/4-Q, and six shorter KTB profiles arranged parallel and perpendicular to the main tectonic lineaments, focussing on the suture between the Saxothuringian and Moldanubian units of the Mid-European Variscides. The Vibroseis method was used throughout the whole reflection survey. In addition, wide-angle observations and two expanding spreads were observed by using explosives. The processing was carried out by the DEKORP Processing Center (DPC) at the Technische Universität Clausthal and, additionally, by various contractors. Standard software was used, and with painstaking diligence yielded remarkable quality results despite the complicated structure of the subsurface. The handling of special problems met within the processing is explained, e.g. offset-restricted velocity analysis, offset-dependent stacking etc.. The results show a very heterogeneous crust with strong reflections distributed over almost the entire crust from surface to Moho level at about 30 km depth. Reflections dipping SE prevail in the middle and lower crust; a thin layer of remarkably high velocity is observed in the central part of DEKORP 4. The complex structure is preliminarily interpreted by a relatively simple model, essentially based on underthrusting of Saxothuringian units under Moldanubian units in the area of Erbendorf. The compressional tectonics has generated wedge-type structures of which the so-called Erbendorf body is of special interest. Moreover, the seismic results clearly show the nappe character of the Münchberger Gneismasse and of the zone of Erbendorf-Vohenstrauß.

Key words: Deep seismic reflection profiling – KTB – Wide-angle reflection profiling – Crustal structure – Wedging – Mid-European Variscides – Moldanubian – Saxothuringian – Erbendorf body

Offprint requests to: C. Reichert

Abbreviations: *DEKORP* Deutsches Kontinentales Reflexionsseismisches Programm; *DPC* DEKORP Processing Center; *KTB* Kontinentales Tiefbohrprogramm der Bundesrepublik Deutschland; *EB* Erbendorf body; *FL* Franconian Line; *LL* Luhe Line; *MM* Münchberg Massif; *MN* Moldanubian; *ST* Saxothuringian; *ZEV* zone of Erbendorf-Vohenstrauß; *ZTM* zone of Tirschenreuth-Mähring; *ZTT* zone of Tepla-Taus; *A* antiform; *S* synform; *LP* low pressure; *MP* medium pressure; *DMO* dip move-out; *NMO* normal move-out; *CSP* common-shotpoint gather; *CMP* common-midpoint gather; *TWT* two-way travel time; *COF* common-offset gather; *LVZ* low-velocity zone

1 Geological aims, planning, field investigations

1.1 Purpose of the investigations; geological situation

The seismic lines discussed in this paper explore a central part of the Variscan Belt of Europe. This belt is more than 1000 km wide and can be subdivided – in the Central European segment – into several zones, which were first recognized by Kossmat (1927). The validity of this zonal scheme has been confirmed by all modern investigations. The zonal boundaries are now regarded as sutures which originated from the closure of several Palaeozoic basins. The opening of most of these basins is essentially related to the break-up of Gondwana during an important rifting episode in Cambrian and Ordovician time. The resulting microcontinental blocks bear witness to a pan-African/Cadomian orogenic event. These microplates (or terranes) were then caught up, during the Devonian and Carboniferous, in the collision between Gondwana and Baltica, which has produced the Variscan Foldbelt. Summaries of this development are available in Weber and Behr (1983), Behr et al. (1984), Franke (1986), Matte (1986a, b), Weber (1986) and Ziegler (1984).

DEKORP lines 4 and 4-Q, as well as the closely related KTB lines 8501–8506, were intended to scan the border zone between the Moldanubian Zone and the northward adjacent Saxothuringian Zone (Fig. 1). The Saxothuringian (ST) represents the infill of a Cambro-Ordovician basin which opened beyond the rift stage at least into a narrow ocean, and the Moldanubian (MN) contains blocks of pre-Variscan crust (and their Palaeozoic cover) which were reactivated by the Variscan orogeny and thrust toward the NW over the Saxothuringian foreland. Tectonic deformation and co-related metamorphism are polyphase and have produced a highly complex crustal structure.

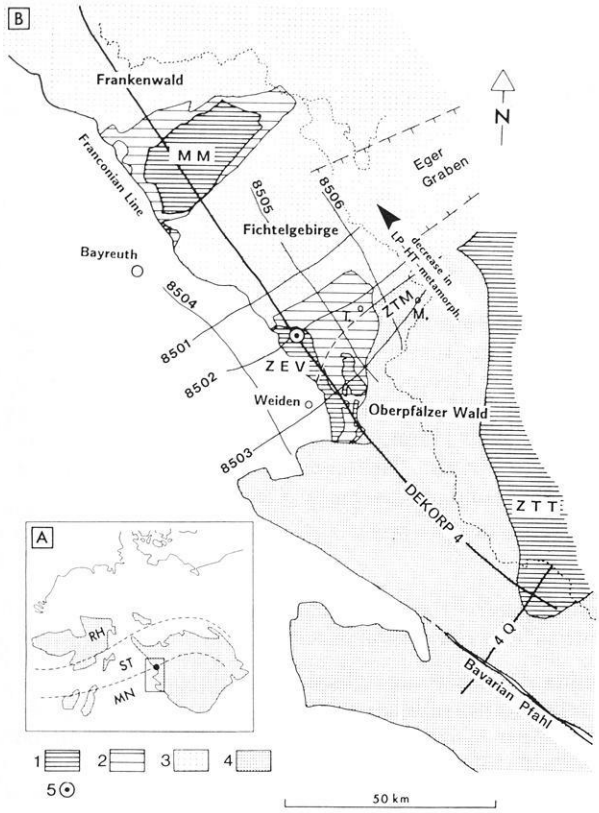

Fig. 1. Geological sketch map of NE Bavaria with the DEKORP-KTB seismic network indicated. **A.** Variscan basement outcrops in Middle Europe with zones after Kossmat (1927). *RH* = Rhenohercynian; *ST* = Saxothuringian; *MN* = Moldanubian. *Inset:* study area with deep drilling site (KTB). **B.** Geological map with main tectonometamorphic units and deep reflection seismic network. 1 = MP metamorphic nappes; 2 = lower nappes; 3 = Saxothuringian; 4 = Moldanubian; 5 = KTB deep drilling site. Late- to post-Variscan granites are not shown. Reflection seismic network: *heavy lines* = DEKORP; *thin lines* = KTB; *T.* = Tirschenreuth; *M.* = Mähring; MM, ZEV, ZTM, ZTT – see list of abbreviations

Saxothuringian (ST) zone

Most of the ST is made up of Precambrian(?) through Lower-Carboniferous sedimentary and volcanic rocks in a conspicuous "Thuringian" facies. Neritic clastics of the Cambrian and Ordovician were probably derived from sources to the NW and, during the Carboniferous, from a tectonic uplift to the SE. A further source area was active, in Givetian and Frasnian time, within the Thuringian basin. Coarse conglomerates are arranged along strike along a line that links areas to the NW of the Münchberg Klippe with the basement uplift of the Saxonian Granulitgebirge, approx. 100 km farther to the NE. This setting suggests an intra-basinal tectonic high along the Granulitgebirge axis.

The key to the tectonic structure of the ST and MN zones lies in a number of medium- to high-grade terranes, set within a major synform (Vogtländische Mulde), where they are in strange contrast with the surrounding sedimentary rocks. These are the metamorphic "Zwischengebirge" of Münchberg, Wildenfels and Frankenberg (the latter two on GDR territory). The metamorphic blocks have alternatively been interpreted as diapir-like uplifts of basement rocks, or as tectonic klippen derived from the MN zone. Recent structural, sedimentological and geophysical studies in the Münchberg area have shown that the metamorphic blocks are truly allochthonous (Behr et al., 1982; Franke, 1984a, b; Haak and Blümecke, 1985).

The Münchberg Massif (MM) comprises the widest lithological spectrum of the "Zwischengebirge" named above. It represents a tectonic pile, in which both the metamorphic grades and the stratigraphic sequence appear in an inverted order (listed here from top to bottom):

1. Gneisses and amphibolites (medium-pressure metamorphism, with kyanite), and some lenses of high-pressure eclogite
2. Epidote-amphibolite
3. Greenschist-grade phyllites and basaltic volcanics
4. Very low-grade sedimentary and volcanic rocks of a conspicuous "Bavarian" facies (the Bavarian sequence, with respect to the Thuringian development, exhibits more deeper-water sediments and a more proximal Carboniferous flysch) subdivided as follows:

- Ordovician sediments with a bimodal suite of intra-plate volcanics
- Silurian and Devonian radiolarian cherts
- Lower Carboniferous flysch

The metamorphic rocks exhibit medium-pressure facies with kyanite. The peak of metamorphism was attained in the early Devonian (at about 390 Ma). Nappe thrusting and very low-grade metamorphism were not terminated before the Lower Carboniferous.

The Münchberg pile of nappes probably originated from an accretionary wedge, which overrode the parautochthonous Thuringian realm from the SE. Since the Saxothuringian rocks of the Fichtelgebirge, to the SE of the Münchberg Massif, are also composed of Thuringian facies rocks, the root zone of the Bavarian facies and the metamorphic units must be sought still further to the SE, i.e. within or at the northwestern border of the MN zone.

"Un-stacking" of the Münchberg pile of nappes and restoring it to a position to the SE of the Fichtelgebirge implies a minimum distance of tectonic transport of the order of 200 km, which testifies to the alpine-type character of tectonic deformation and crustal structure in the target area, and justifies plate-tectonic interpretations (see below).

NW-directed tectonic transport is also documented, at outcrop scale, by NW-verging folds and by numerous thrusts (brittle as well as ductile). All these features represent the first of the six deformation phases D_1, . . ., D_6 of the Variscan orogeny (see KTB, 1986, p. 19).

A second phase has produced more open, SE-verging folds and thrusts. A third phase, which is clearly detectable only in the Fichtelgebirge, led to the formation of still more open, upright folds with a steep crenulation cleavage (Stein, 1987).

At map scale, the structural pattern is dominated by a number of major synforms (S.) and antiforms (A.) which originated during the later stages of tectonic deformation. These are, in order from NW to SE: Schwarzburg A., Teuschnitz S., Berga A., Vogtland S. (which contains the "Zwischengebirge" klippen), Fichtelgebirge A. and Hatzenreuth S. (Figs. 1 and 2).

With the exception of the Münchberg Klippe, most of the Saxothuringian rocks are of low to very low metamorphic grade. Greenschist facies rocks occur only in a transverse zone with enhanced heat flow to the NE of the MM (Franke, 1984a, b) and in the core regions of the Fichtelge-

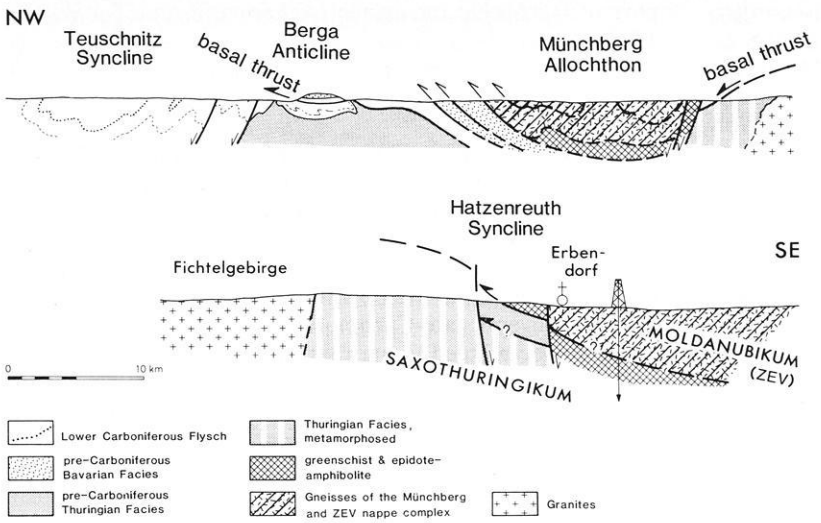

Fig. 2. Geological cross-section through the Oberpfalz area (NW–SE)

birge A. (staurolite-andalusite, Mielke et al., 1979). For reviews of the metamorphic development in the target area, see Blümel (1985), KTB (1986, p. 14), and Schüssler et al. (1986).

Saxothuringian/Moldanubian boundary region

The structure of the ST/MN boundary region is difficult to assess because it is intruded by important volumes of post-tectonic granite and because NW/SE block-faulting has brought to the surface very different levels of the tectonic structure. Individual segments of the boundary (the so-called "Erbendorf Line") probably differ in their origin.

North of Erbendorf, near the western margin of the basement outcrop, Thuringian facies rocks at the SE flank of the Fichtelgebirge A. are bounded by a SE-dipping thrust fault. Very low-grade Devonian sediments are overthrusted by greenschist facies volcanics and lenses of serpentinite which closely resemble the Münchberg greenschists. This is especially true of their petrological affinities (calcaline in both areas, see KTB, 1986, p. 27). The greenschists, in turn, are overlain by gneisses and amphibolites of the Erbendorf-Vohenstrauß Zone (ZEV). The ZEV rocks exhibit the same metamorphic facies (medium-pressure with kyanite) and the same metamorphic ages as the Münchberg gneisses (KTB, 1986, p. 14; Schüssler et al., 1986). Hence, the greenschists and gneisses at Erbendorf must be regarded as equivalents of the respective units at Münchberg, preserved in a position closer to the root zone. The Bavarian facies Palaeozoic rocks appear to pinch out toward the SE, since they are reduced in thickness at the SE margin of the Münchberg Klippe, and are no longer detectable at Erbendorf.

East of the Steinwald granite, in the Tirschenreuth-Mähring area, the ST/MN boundary is less evident. As already recognized by Schreyer (1966), and reaffirmed in much more detail by Wagener-Lohse and Blümel (1986), Stein (1987) and de Wall (1987), there is a continuous metamorphic transition from the chlorite-bearing schists of the Hatzenreuth S. towards the SE through the cordierite/K-feldspar gneisses of the Moldanubian proper. As in the Fichtelgebirge, the metamorphic facies is of the low-pressure type. Though the northern part of the MN is affected by a broad subvertical zone with high-temperature mylonites (KTB, 1986, p. 21), the sequence of southward-increasing metamorphic grades is complete.

Hence, the ST/MN is difficult to define, and, from merely lithological aspects, the Moldanubian gneisses might just represent Saxothuringian Palaeozoic rocks of higher metamorphic grade. However, geochronological studies (KTB, 1986, p. 32; Teufel, 1987) have revealed traces of an older metamorphic event in the Moldanubian gneisses. Besides, there are relics of a medium-pressure metamorphic event which pre-dates the low-pressure metamorphism of the Moldanubian proper.

Hence, the Moldanubian rocks east of the Steinwald granite must be regarded as part of a separate tectonic entity, with an older and more complex tectono-metamorphic history, which was brought into tectonic contact with the ST rocks of the Fichtelgebirge and then was welded together with these during the subsequent low-pressure metamorphic event. The latter is dated at about 330 Ma, i.e. at about the Lower/Upper Carboniferous boundary (Teufel, 1987).

In summary, it is obvious that the ST/MN boundary in the Tirschenreuth-Mähring area is of great structural importance, though its exact position and significance are still being debated (see Section 5). It can be stated, however, that the Tirschenreuth-Mähring area represents a deeper structural level than that exposed at Erbendorf.

Moldanubian (MN) zone

Most of the MN region in Bavaria, Czechoslovakia and Austria is made up of metapsammitic and metapelitic gneisses with some intercalations of graphitic schist and marble. This association (the MN proper) has been further subdivided into lithological units and compared with Precambrian sequences elsewhere; at least part of the metamorphic alteration has been attributed to a Cadomian event (Stettner, 1981). However, recent isotopic studies (KTB, 1986, p. 32) have yielded Palaeozoic metamorphic events, and new palaeontological evidence has revealed the presence of Cambrian and Silurian sediments among the MN metamorphic sequences (KTB, 1986, p. 15). The history of the MN zone will have to be re-assessed with modern methods of investigation.

The MN proper has been affected by the same low-pressure metamorphism as the ST rocks of the Fichtelge-

birge to the north, but exhibits higher grades up to cordierite/K-feldspar. Accordingly, radiometric dating has revealed the same age as in the north (approx. 330 Ma; KTB, 1986, p. 32). Some relic minerals give evidence of an earlier medium- and high-pressure metamorphic event (probably around 390 Ma). Further to the SE, in the Bavarian Forest, there are indications of a still older anatectic event dated at about 460 Ma (Grauert et al., 1974).

The MN proper is structurally overlain by a sequence of gneisses with numerous inserts of amphibolite, which outcrops along the western margin of the Bohemian basement block and has been termed the "Zone of Erbendorf-Vohenstrauss" (ZEV) after two towns at its northern and southern margins. A direct equivalent of the ZEV rocks, in terms of lithology as well as of metamorphic character, is exposed to the east of the MN proper: the gneisses of the "Tepla-Taus Zone" (ZTT) in Czechoslovakia, which forms the western part of the extensive Tepla-Barrandean block, the core of the Bohemian crystalline massif.

ZEV and ZTT both exhibit medium-pressure metamorphic facies, without clear indication of a younger low-pressure event. Hence, it could be concluded that they occupied a higher and therefore cooler structural level during the time of low-pressure metamorphism. Alternatively, they might have been emplaced after the low-pressure metamorphic event. In most of the area, the contact between the overlying units is obscured by granites or younger block-faulting. It is at the SE border of the ZEV only, that a ductile mylonite zone can be observed.

Anyhow, the ZEV rocks must be regarded as an equivalent of the MM gneisses since they exhibit similar lithologies (with frequent mafic intercalations), the same medium-pressure metamorphism and also the same metamorphic age (approx. 390 Ma; KTB, 1986, p. 32), thus providing further evidence of the allochthonous nature of the MM.

The MN proper exhibits the same sequence of deformational events as does the Saxothuringian to the immediate north (KTB, 1986, p. 19). The peak of low-pressure metamorphism, in the MN rocks, occurred in an early stage of the D_3 deformation. The metamorphic isograds were still folded around the ENE-trending D_3 fold axes, and, later, around a NS-oriented set of D_4 structures. A major D_4 antiform is responsible for the outcrop of the MN proper between the cover sequences of the ZEV (to the west) and the ZTT (to the east).

The ZEV rocks were not perceptibly heated during the low-pressure event and do not show, therefore, the synmetamorphic fabrics and structures acquired by the MN rocks. They exhibit, instead, a complex set of structures related to the earlier medium-pressure event (which, in turn, is not detectable in the low-pressure MN rocks proper).

Variscan granites

The central and southern parts of the target area are intruded by an important volume of post-tectonic granites. Their intrusion ages range from approx. 320 to 280 Ma (Besang et al., 1976; Köhler and Müller-Sohnius, 1976; Lenz, 1986; Richter and Stettner, 1979). One larger group of granites occupies the core of the Fichtelgebirge A. (D_3). Other granite bodies appear to follow NW/SE-oriented fracture zones. In the Flossenbürg and Bürgerwald granites (both within the MN zone), the spatial array of trace-element zoning suggests plate-like bodies which are probably part of laccolithic intrusions (Ackermann and Tavakkoli, 1986).

Post-Variscan structures

The NW/SE alignment of some of the granites reflects a system of block-faults which was formed in Upper Carboniferous-Permian time and reactivated repeatedly until recently. One of these faults is the "Franconian Line" (FL) (Fig. 1), along which the Mesozoic and Tertiary rocks of the western foreland are downfaulted locally for more than 1000 m. Several late-Carboniferous/Permian depocenters appear to be aligned along that fault (e.g. Emmert, 1981), and it is possible that these basins represent pull-apart features associated with dextral strike-slip movements like those proposed by Arthaud and Matte (1977).

The main movement along the NW/SE faults, at least during Mesozoic and later times, is a more or less vertical downthrow to the SW. This is also evident from another important fault zone which runs from Bad Berneck (in the NW) to Pleystein (in the SE) at an acute angle with the FL, both including a narrow segment of basement rocks between them at the western margin of the Bohemian Massif. The site of the German continental drilling (KTB) lies within that segment. The Kulmbach Fault, which parallels the FL within the Mesozoic foreland is another example of the same kind of fault.

The FL, as well as the Bad Berneck-Pleystein fault, dips steeply (70°–80°) to the NE, as is observable in surface outcrops. This might be due to gravitational spreading, at near-surface level, of the uplifted basement rocks and their encroachment upon soft Mesozoic foreland rocks, or else reflect a compressive tectonic regime.

Another important NW/SE element is the Bavarian "Pfahl" (Fig. 1), a dextral shear zone with cataclastic as well as ductile deformation and extensive quartz mineralization, which was still active in Triassic time (Horn et al., 1983). A similar quartz vein, the Bohemian "Pfahl", occurs close to the east of and parallel with the western margin of the ZTT (in Czechoslovakia).

One of the youngest tectonic elements is the Eger Graben (Fig. 1), which roughly follows the ST/MN boundary along approx. 200 km. It is characterized, in the target area, by local cover of Miocene sediments and by a number of basaltic pipes and lava flows of the same age, which can be traced across the FL into the Mesozoic foreland.

Purpose of survey and objectives of the seismic lines

The objective of the survey was the investigation of the crustal structure of the ST and MN zones, with special emphasis on the boundary region which was under consideration and has since been selected as the well site of the Continental Deep Drilling Project (KTB). The long profile, DEKORP 4, was intended as a general cross-section from the Teuschnitz S. in the north to the MN rocks in the south. The KTB lines 8501–8506 were arranged in the form of a grid to explore the ST/MN boundary region near Erbendorf (i.e. around the KTB drilling site). This array of lines (Fig. 1) represents a first step in obtaining a 3-D view of the target area.

The DEKORP 4-Q line is positioned at a right angle with respect to the DEKORP 4 line near its southern end. Line 4-Q runs across the regional tectonic trend of the Ba-

Table 1. Important data of the Oberpfalz survey 1985

Profile	Length	Source parameters for accompanying investigations	
DEKORP 4	186.88 km	Number of shots:	96
DEKORP 4-Q	36.64 km	Drilling rigs:	6
KTB 8501	47.44 km	Drilling depth:	30 m
KTB 8502	50.48 km	Boreholes per shot:	3
KTB 8503	56.80 km	Charge per shot:	90 kg
KTB 8504	50.72 km		
KTB 8505	54.80 km		
KTB 8506	42.60 km		
Total	526.36 km		

varian Forest (NW/SE) and was intended to explore important tectonic structures such as the Bavarian "Pfahl" and the western margin of the Tepla-Taus Zone (ZTT), which is marked, in this area, by an important volume of mafic metamorphic rocks (Hoher Bogen).

Lines KTB 8505 and 8506 were arranged to explore the Tirschenreuth/Mähring segment of the ST/MN boundary region. The Erbendorf segment is crossed by the main DEKORP 4 line. KTB 8504 is situated in the Mesozoic foreland, in an area which is probably underlain by a westward continuation of the Erbendorf-Vohenstrauss Zone (ZEV).

While the above lines yield cross-sections with resepct to the main tectonic trend (SW-NE) in the area, lines KTB 8501–8503 are arranged parallel to strike, but cut across the NW/SE-directed system of block-faults at the SW margin of the Bohemian Massif. These faults were expected to produce important steps in the reflection surfaces, even at greater depths.

1.2 Field technique

In order to accomplish a highly effective seismic reflection investigation, the survey of lines DEKORP 4 and 4-Q was carried out together with that of the six KTB lines in a joint field survey. Thus, uniform field parameters were chosen to allow a good comparison. Another important measure was the integration of wide-angle observations and expanding spread arrangements in the survey. This work was only partly carried out by the contractor, Prakla-Seismos AG: a great deal was taken over by crews from the universities and geological surveys with their own equipment. For this reason, explosives had to be used to provide a suitable energy source. Important data of the Oberpfalz survey 1985 are listed in Table 1.

In contrast to the DEKORP 2-South survey (DEKORP Research Group, 1985) where Mesozoic and Cenozoic sediments represent the prevailing outcrops, in the Oberpfalz pre-Permian metamorphic and crystalline rocks are present at the surface. This had an important influence on the decision of whether explosion seismics (as on DEKORP 2-South) or Vibroseis should be used; due to the difficulty in estimating the drilling progress, the Vibroseis method was chosen. This decision was also justified by the very good experience in surveying the Schwarzwald area in 1984 (Lüschen et al., 1987).

Hence, the field parameters were derived from experience of the former surveys. Regarding the geometry, two facts were decisive: a sufficiently high degree of coverage in the shallow subsurface should be reached and an adequate long offset should provide enough normal move-out for safe calculation of velocities. These considerations resulted in a compromise: an asymmetric split-spread with 4-km and 12-km spreads. A list of the parameters used is given in Table 2.

Table 2. Field parameters for the near-vertical seismic reflection survey in the Oberpfalz 1985

Method	Vibroseis
Equipment	SERCEL SN 368, telemetric, 200 channels
Sampling rate	4 ms
Sweep	12–48 Hz upsweep
Sweep length	20 s
Listening time	12 s
Record length	20 s + 12 s = 32 s
Filters	12 Hz, 18 dB/oct; 89 Hz, 72 dB/oct
Number of geophone groups	200
Geophone group interval	80 m
Geophone pattern	24-fold, in-line
Pattern length	80 m
In-line offset	200 m
Geometry	asymmetric split-spread 4.12 km – 0.2 km – VP – 0.2 km – 12.12 km
Number + type of vibrators	5 VVEA, 16 tons peak force
Vibrator pattern length	145 m/49 m
Vibrator point interval	80 m
Vertical stacking	10-fold
Coverage (ideal)	100-fold
Mean coverage (actual)	75-fold

2 Data processing

2.1 Processing by the DEKORP Processing Center (DPC)

The processing was carried out by the DPC at Clausthal with the Raytheon RDS 500 and VAX 11/750 computers and standard software of Seismograph Service Ltd. In DEKORP Research Group (1985) the single processing steps were described in detail. The aim of this section is to emphasize the peculiarities of the processing of the Oberpfalz data.

CMP processing and stacking

The demultiplexed common-shotpoint gathers (CSP) were rearranged into common-midpoint gathers (CMP). Due to unavoidable lateral offsets (up to 1 km) and crooked-line field configurations, there was a strong scattering of the source-receiver midpoints. Thus, a processing line with CMP intervals of exactly 40 m was calculated and the corresponding traces were related to these points.

The following steps were optimized by special analyses. First, the strong energy decrease within the first seconds was compensated by an analytic gain function. Then, basic static and dynamic corrections, muting and scaling by AGC were applied. Subsequently, a brute stack was performed in order to facilitate a quick overview over all profiles. This stack was obtained by use of only a few velocity analyses and one single muting curve. Finally, the data were bandpass filtered. In order to obtain the final stack a large

number of specialized analyses regarding the respective processing parameters were performed, resulting in an improved resolution.

Special emphasis within the CMP processing was given to the assessment of NMO velocities derived from constant-velocity stacks. At 7–10 points per 50 km profile, test stacks were performed with about 30 constant velocities within groups of 20 CMPs. The evaluation of these velocity scans resulted only rarely in unambiguous velocity – TWT functions, i.e. coherent stacking at a particular reflection time is possible over a broad velocity range (DEKORP Research Group, 1985). This might be due to complicated geological structures on the one hand (e.g. different dips at the same travel time necessitating different NMO velocities) and, on the other hand, due to effects of seismic imaging at greater travel times (e.g. increasing spatial influence of diffractions with increasing travel times).

In order to identify the influence of lateral velocity variations, offset-restricted test stackings (30 constant velocities, five offset ranges) were performed in the centre area of profiles DEKORP 4 and KTB 8502. The stacking results were quantitatively equivalent for all offset- and time-domains within a broad velocity range, thus excluding a detailed analysis of lateral velocity variations. Therefore, only one velocity-time function was applied for ten different offset-domains of the respective central line parts mentioned before.

The results (Fig. 3) show that the different offset ranges contribute partial information to a complete image of the subsurface. The stack of small offsets (up to 4 km) evidences good reflections at 3–4 s TWT in the marginal domains of this part of the section: the central domain is more or less void of reflections. On the other hand, the stacks of the greater offsets (4.0–8.0 km and 8.0–12.0 km) give good reflections in the central part, the quality of reflections becoming poor in the marginal domains.

Three conclusions can be drawn from these results:

1. All offset domains produce different, but equally important, contributions to the final result.

2. The differences can be explained – at least partly – by the inhomogeneous overburden.

3. Generally, the signal/noise ratio is not as much improved with increasing coverage as expected.

In order to support better interpretation, the complete DEKORP 4 profile was stacked additionally with drastically increased velocities emphasizing strongly dipping reflections. Furthermore, the complete KTB 8502 profile was stacked using only offsets up to 4 km.

Automatic residual static corrections and coherency filtering

An essential improvement in processing the Oberpfalz data was obtained by calculation and application of residual static corrections before stack and by coherency filtering after stack. This procedure improved, in broad areas, the content of information and the resolution of the sections. For this reason a short description of these two time-consuming processing steps is given in the following.

Experience shows that static corrections calculated from short refraction lines and/or first arrivals of the reflection records are not sufficiently precise in most cases. Therefore, residual statics had to be assessed. This was done by the DPC using two independent algorithms.

The first method calculates surface-consistent residual

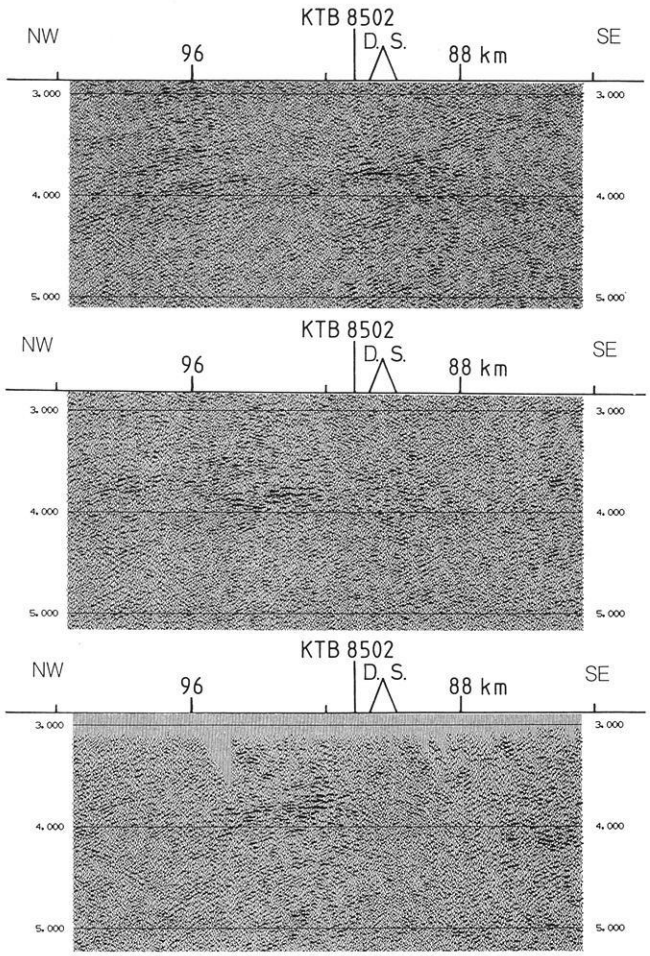

Fig. 3. Profile DEKORP 4: stacks of the offset domain up to 4 km (*top*), 4–8 km (*centre*) and 8–12 km (*bottom*) from the part including the Erbendorf body. *D.S.* = drilling site

static corrections for particular source and receiver positions under the assumption that near-surface influences (e.g. variations in altitude, thickness of the weathering layer and velocity) generate pure time shifts (neglecting the other parts of the ray paths). That is, a given surface position correlates with a constant time shift. The residual statics are calculated in two phases:

1. Estimation of relative time shifts by cross-correlation of dynamically corrected CMP traces with model traces

2. Calculation of source and receiver statics by the Gauss-Seidel iteration method (Taner et al., 1974)

The second method calculates subsurface-consistent residual static corrections for each CMP trace. The relative time shift of the respective trace is calculated by cross-correlation with a pilot trace obtained by weighted stacking of several adjacent CMPs. Up to two maxima of the correlation function are considered, provided that the second maximum exceeds a selected relative threshold value. Three cases have to be distinguished:

1. Only one maximum is found – its delay is taken as residual static value.

2. Two maxima fulfil the conditions – the correct value will be found by trial-and-error application and comparison with the pilot trace.

3. No unambiguous maximum is found – the residual static value is set equal to zero.

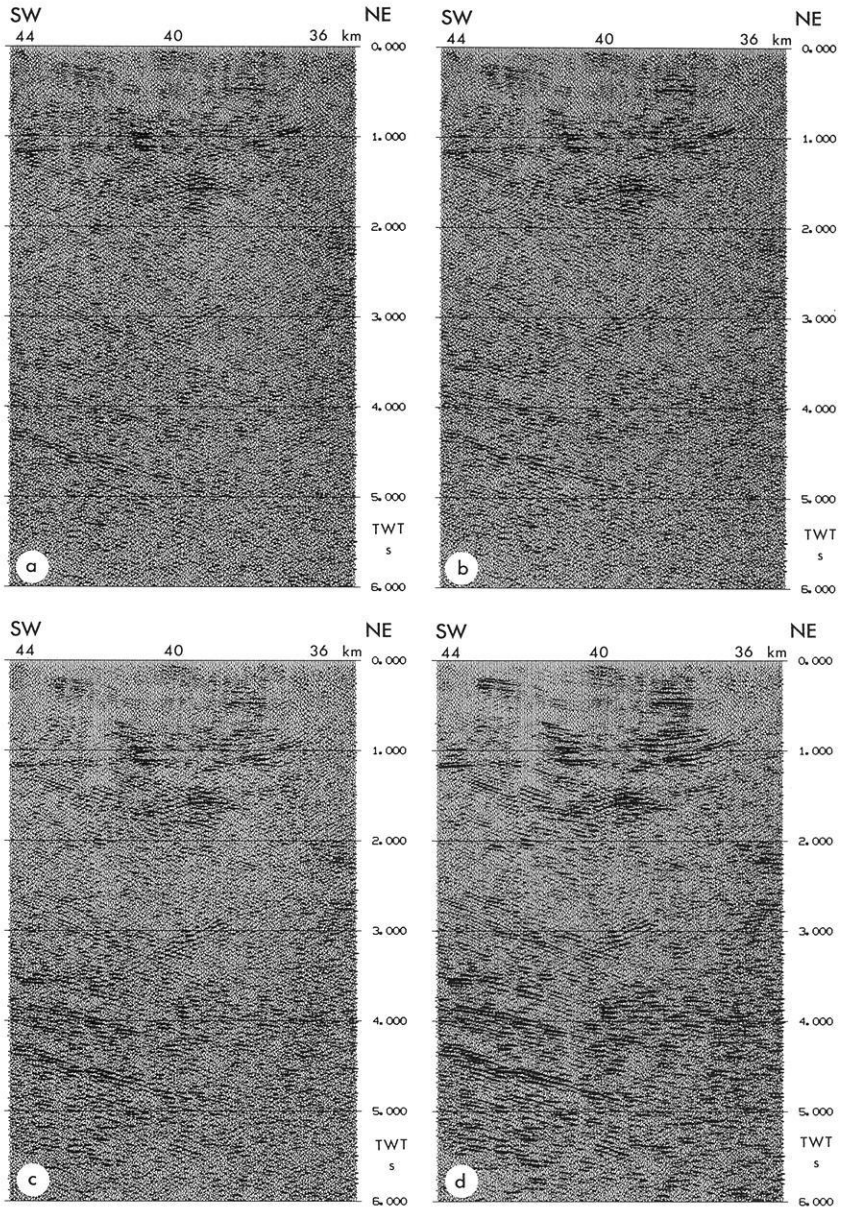

Fig. 4a–d. Example for the improvement of results by applying automatic residual static corrections and coherency filtering:
a original section;
b with surface-consistent corrections;
c with surface- and subsurface-consistent corrections;
d with the same corrections as in **c** and subsequent coherency filtering

In both methods, surface- and subsurface-consistent residual statics, a certain maximum shift must not be exceeded (typically 20 ms). The efficiency of both methods is demonstrated in Fig. 4a–c and it is obvious that, with successive application, each of them produces an equivalent improvement.

Coherency filtering represents, especially in deep seismic profiling, a useful procedure for improving the clarity of the sections. This procedure was applied to stacked sections in order to suppress incoherent noise and to increase the amplitude of reflections extending over a number of traces. The procedure works as follows: trial stacks of a number of adjacent traces over a given window and along straight lines with a variety of different slopes result in summed trace windows. That one with maximum energy is chosen as part of a coherency trace. This part is added with a weighting factor to the centre trace of the original input, resulting in a coherency-filtered trace for the selected time window. Repeating this procedure for all time windows and for all traces yields the coherency-filtered section. Figure 4d shows an example. It has to be mentioned that only particular linear alignments will be emphasized due to the prevailing dip within the respective window. By suitable choice of window lengths, number of traces and weighting factors, this disadvantage can be avoided.

Coherency filtering improves the display of the sections, emphasizing general trends and structures provided that the parameters are chosen carefully. If not, reflections may even be weakened. Nevertheless, a careful comparison with the unfiltered data is necessary. Under such precautions coherency filtering provides a useful tool for increasing the readability of deep seismic data.

Migration

Usually, the finite-difference (FD) migration is applied because velocity variations in all directions are permitted and an optimum signal/noise ratio is obtained. In order to diminish the processing time, the data were resampled at 8 ms sampling interval under the condition that fatal deviations

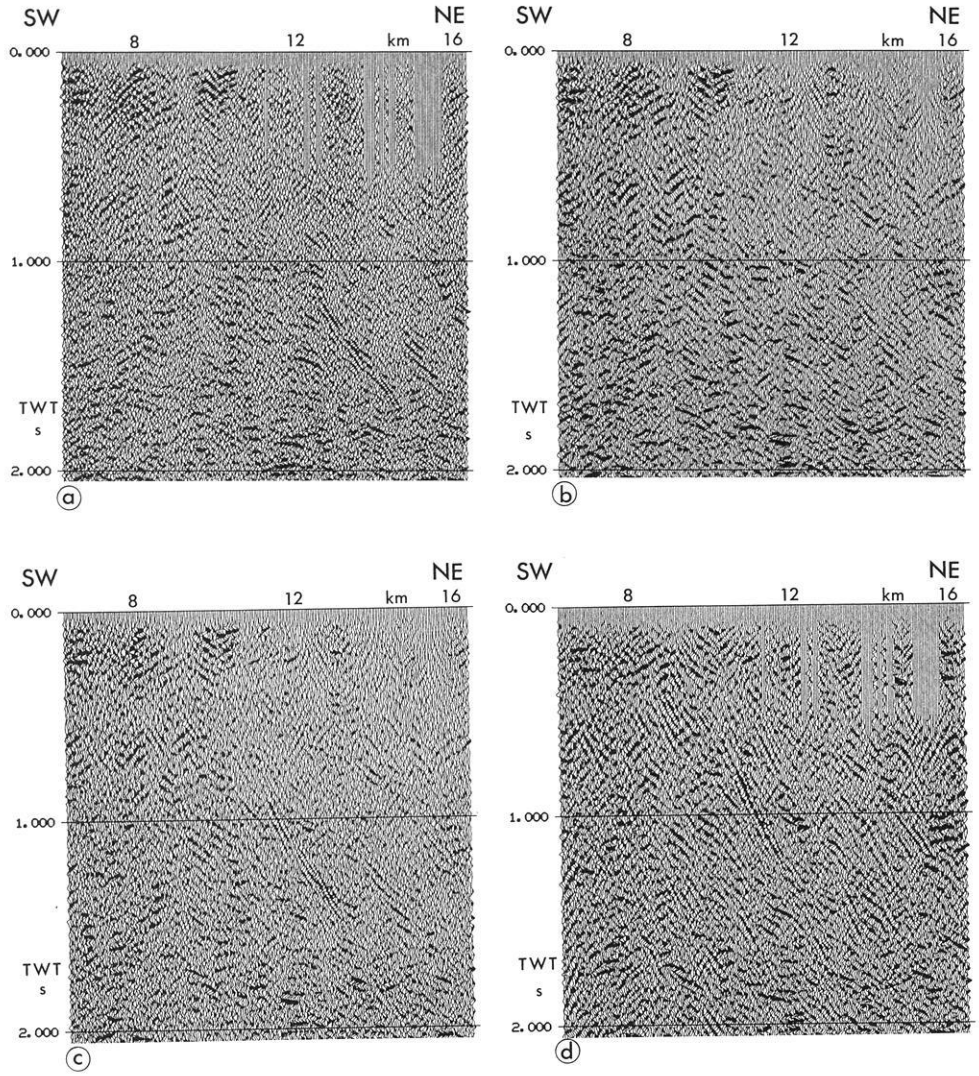

Fig. 5a–d. Stack of a part of profile DEKORP 4-Q
a unmigrated, **b** FD migrated, **c** FK migrated and **d** Kirchhoff migrated. The migration velocity at 1 s TWT was 3825 m/s

due to frequency dispersion can be excluded. Figure 5a shows a part of the DEKORP 4-Q profile and Fig. 5b the corresponding FD migration. From inspection of the steeply dipping structure of the Bavarian "Pfahl", it is obvious that the migration is strongly affected by dispersion. In order to reduce this effect the following procedures can be applied:

1. Resampling input data at smaller sampling intervals
2. Using smaller downward continuation steps
3. Decreasing the spatial sampling interval by interpolation

All these steps have the disadvantage of a strong increase in processing time. Therefore, other migration methods could be suitable. The frequency-wavenumber (FK) migration and the Kirchhoff migration were at hand.

The fast FK migration does not lead to dispersion effects (Fig. 5c): the data can be migrated over a wide range of dips (this was also tested by the use of synthetic data). It is well known that this method is not suitable for providing final sections with complicated structures because it works only very unprecisely in the presence of velocity variations. However, due to its speed, this method is well suited to estimating migration velocities (focussing of diffractions). For this purpose trial migrations are performed with different velocities, finally choosing that migration velocity which makes the diffractions contract to an area of minimum width.

The Kirchhoff migration works well in the presence of steep dips and variable velocities. In principle, this method migrates all dips correctly without remarkably increased processing time. But the result was often not clear, due to a bad signal/noise ratio (Fig. 5d).

Therefore, all final migrations were obtained with the FD method, using decreased, smoothed stacking velocities and additional velocity information from refraction seismics.

All migrations, especially of short profiles, are strongly affected by boundary effects. The amplitude energy of the marginal traces will be smeared along half-circles, the radii of which are the two-way travel times of these traces. This effect can be reduced by horizontal tapering of these traces. Best results have so far been obtained using synthetic data. This method has also been tested on real data, but additional efforts are necessary for further improvement.

Remarks

During the work we have tried to answer the question of whether deconvolution can contribute to a contraction of events in Vibroseis data. For this purpose, zero-phase wave-

lets were transformed into minimum-phase wavelets and a standard deconvolution was applied. These tests succeeded in several areas and the results encourage further efforts.

In order to obtain additional information about the subsurface lithology, instantaneous frequencies were calculated by Hilbert transforms in the centre parts of profiles DEKORP 4 and KTB 8502. But this method, which is often successful in exploration seismics, failed in this case. This might be due to the frequency limitation of the applied Vibroseis signals.

Finally, it should be mentioned that the processing of the DPC so far has been performed nearly exclusively with a standard software package. The demand for better adaptation of some subprograms to the problems of deep seismic profiling or for replacing them entirely became more and more evident.

2.2 Processing by companies

Five of the six KTB lines were given to four contractors with the intention of getting final processing of these lines within the limited time to prepare the decision on the location of the KTB and to test the results of different kinds of modern processing simultaneously: Compagnie Générale de Géophysique, Massy, France; Prakla-Seismos AG, Hannover, Germany; Preussag AG, Hannover, Germany; Seismograph Service Ltd., Keston, Great Britain. The companies were provided by DPC with already preprocessed data and with brute stacks of their respective profiles in order to try further improvements.

The results of the different processing sequences can be compared only with care because the procedures were applied to different profiles. Together with the brute stacks of all profiles from DPC, some conclusions may be drawn.

The most important distinctions resulted from different procedures to obtain residual statics, from offset restrictions and DMO processing (dip move-out). Residual statics provided a remarkable improvement, regarding the resolution and strength of reflections. However, special care should be taken in choosing methods and parameters. Strong improvement and a smoothing effect is obtained for long continuous Palaeozoic reflectors within sedimentary portions. On the other hand, short and weak events above and beneath these reflectors are not improved, but rather destroyed. Moreover, it is not proved that the reflectors are as smooth as they appear after application of these methods. A combination of surface-consistent and CMP-consistent residual statics seems to provide a more balanced result.

Offset restriction is an ambiguous method. A certain clarification of reflection patterns in very complicated domains was obtained, but it has to be kept in mind that in such cases some information is neglected. This became obvious when stacking tests with different offset domains were performed at the DPC (cf. Section 2.1).

DMO or partial pre-stack migration is a useful method in regions with complex geology. The data are dip-dependently corrected by DMO so that subsequent dynamic corrections can be applied using a unique velocity field. This method provides a better fit to the actual subsurface parameters (i.e. velocities and dip angles). Although the resulting section does not look much different from that without DMO, the velocities obtained from this method are more consistent and better suited to discussing geology than those determined by routine velocity analyses which sometimes lead to unrealistically high values. Velocity-depth functions derived from this method along profile KTB 8506 are presented in Fig. 26.

It can be concluded, that special processing has advantages and disadvantages and the results have to be regarded carefully. Even the brute stacks of all profiles, as provided by the DPC, show that a cautious and experienced way of choosing the processing parameters yields sections which are qualitatively comparable to the final stacks provided by the companies.

3 Results of the near-vertical seismic reflection survey

All along DEKORP 4 a great number of reflections were recorded in the upper as well as in the lower crust. This long profile, which runs perpendicular to the general Variscan strike, represents a key to the structural character of the area under investigation. The description of this profile will serve as an introduction to the network of the other lines.

3.1 DEKORP lines 4 and 4-Q

A line-drawing showing the whole migrated DEKORP 4 profile is presented in Fig. 6. Parts of the migrated section are reproduced in Figs. 7–11 and 13–16. The description starts in the Saxothuringian (ST) part (NW) continuing to the Moldanubian (MN) domain (SE).

Figure 7 shows strong horizontal reflectors at approximately 1 s TWT to be correlated possibly with Upper Devonian spilites of Frankenwald. Underneath, several subhorizontal bands of reflections appear down to about 6 s TWT. The lower crust shows only poor reflections (Figs. 6 and 51). But at its base the Moho is relatively strongly reflecting at 10.0–10.5 s TWT. This result is typical for the entire northern part of the profile. This image is in contrast to the southern part of the profile where strong reflections are observed both in the upper and in the lower crust. The results obtained along the entire DEKORP 4 profile represent a pronounced contrast to the so-called "typical continental crust", i.e. poorly reflecting upper crust and highly reflecting "laminated" lower crust (e.g. Meissner et al., 1982; Lüschen et al., 1987; Matthews and Cheadle, 1986; Matthews et al., 1987; McGeary, 1987).

Just below the base of the Carboniferous in the SE a wide antiformal structure is visible between 1.5 and 2.0 s TWT (Figs. 7 and 8). It can be correlated with surface structures, the Berga A. and the Hirschberg A.. Other strong reflections can be observed down to 5 s TWT.

Following in the SE, a bowl-type structure appears in the uppermost crust with its deepest point at about 1.3 s TWT (Fig. 9). It represents the base of the Münchberg Massif (MM) between 130 and 155 km. This finding is an additional piece of evidence that this unit is to be interpreted as a nappe. Further to the SE another antiformal structure is observed at a level of less than 2 s TWT at about 120 km (Fig. 10). It is located below the Fichtelgebirge A.. Parallel reflections are seen down to 4.5 s TWT.

In the centre of the DEKORP 4 profile (Fig. 11) there is a zone of prominent reflections in the upper crust at about 3–4 s TWT. This zone has been observed along all NW/SE-running profiles and its basal zone coincides, along

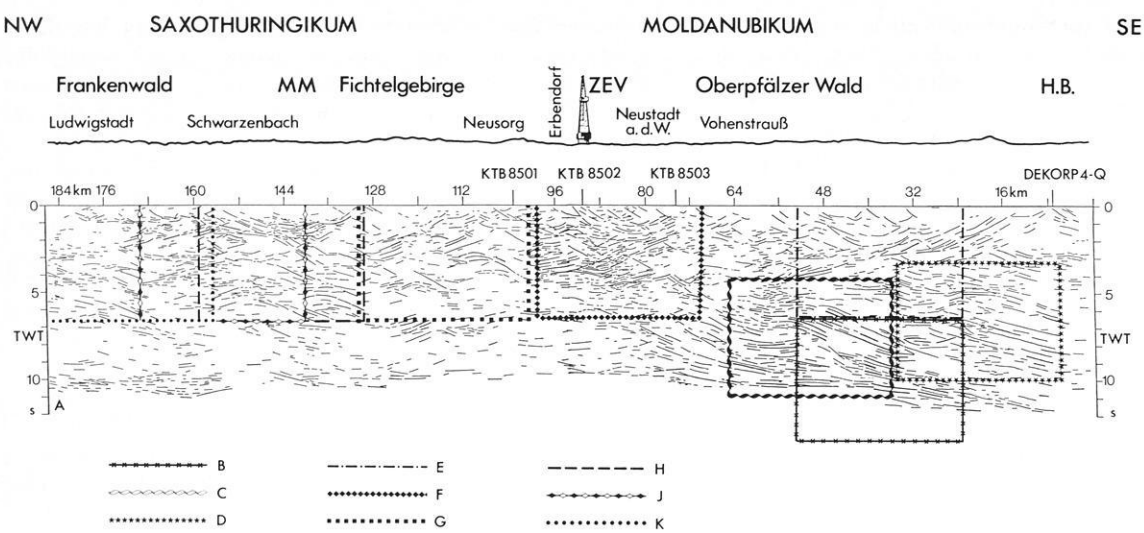

Fig. 6. Profile DEKORP 4: line-drawing of the migrated section. *Frames* indicate that part of the section which is given in more detail be a following figure, denoted by the corresponding letter

DEKORP 4, with a wide-angle reflector of abnormally high *P*-wave velocity material (Section 4.2). It has a wedge-type imbrication structure and overrides a SE-dipping band of reflectors which combines 50 km further to the SE with the Moho discontinuity. This imbricate structure will be called "Erbendorf body" (EB) in the following. The internal structure of the EB shows NW-dipping reflectors reaching, in many cases, up to the SE part of the base of the ZEV.

The strength of the reflections decreases remarkably below the EB. This might be due to a certain shielding effect of the EB. The wide-angle observations show clear and continuous Moho reflections below the EB and some subhorizontal reflections in the lower crust (Section 4.2).

Above the EB a bowl-type structure is seen (Figs. 6 and 11) which should be related to the base of the nappe complex of the ZEV at about 2 s TWT, corresponding to 5–6 km depth.

At the NW rim of the ZEV and at the adjacent greenschist zone, various fault systems with more or less E–W strike are observed at the surface. They might be an explanation for a particular phenomenon which became evident from stacking with different offset ranges (Section 2.1, Fig. 3). These near-surface inhomogeneities seem to dissipate seismic energy for certain domains at greater depth (Fig. 12). Analysing the results in more detail, a dependence on ray directions seems to play a role: rays travelling more or less parallel to these fault systems are disturbed more strongly than those rays travelling only a short distance perpendicularly through that zone. Presumably, these effects are not restricted to the afore-mentioned area and additional efforts should be made in order to investigate this problem more precisely.

Between the base of the ZEV and the top of the EB a complicated pattern of reflections is seen with different directions of apparent dip. Figure 13 presents the SE continuation of the above-mentioned strong band of reflections which might be a master décollement. It is best seen from about 6.5 s TWT at the NW edge of the figure to about 9.3 s TWT at the SE edge, forming a ramp-like structure in its middle part. A broad band of parallel reflections of about 1.5 s width is situated above this ramp-like structure with its top culminating at about 5.5 s TWT. Above the culmination point there seems to be a structural discontinuity at approximately 4.8 s TWT, indicated by subhorizontal reflections extending from about 48 km to the SE end of Fig. 13. Below the ramp-like structure at 8.0 s TWT, a lens of strong reflections is visible from 54 to 60 km. At greater depths the reflections appear dipping weakly to the SE. The Moho is shown by clear subhorizontal reflections at about 10.2 s TWT.

Also in the upper crust good reflections appear as shown in Fig. 14. It shows subhorizontal reflections in its SE part between 2.6 and 5.0 s TWT. The subhorizontal reflections at 4.8 s TWT represent the afore-mentioned structural discontinuity. They are cut off by a strong band of NW-dipping reflections from 2 s in the SE to 4 s TWT in the NW. Their possible origin will be discussed in Section 5.

Further to the SE, Fig. 15 shows the continuation of the structural discontinuity. At about 20 km it bends down from 4.8 s to about 6.0 s at the SE end of the figure. Below the bending point another culmination of reflections appears at about 24 km and 6.5 s TWT; it is similar to that observed at 56 km. These findings reveal significant characteristics of the tectonic structures along DEKORP 4. It seems that SE-dipping elements and ramp structures are typical properties of the crust in this region.

Figure 16 shows remarkable features of the Moho level in the southern part of DEKORP 4. In the left and centre parts of the figure the Moho shows very strong subhorizontal reflections at about 10.0–10.5 s TWT. Distinct phases are observed correlating over long distances. At 36 km, however, the Moho bends down and dips SE down to about 11.5 s TWT where it cannot be followed further due to the restricted record length of 12.0 s. This corresponds to 34.5 km depth assuming a mean crustal velocity of 6.0 km/s.

Profile DEKORP 4-Q is situated at the SE end of DEKORP 4 and runs perpendicular to the NW–SE strike of the gneisses at the SW margin of the Bohemian Massif ("Bavaricum"). For its line-drawing see Fig. 17. At its NE end it crosses the Hoher Bogen – an amphibolitic nappe – belonging to the allochthonous Tepla-Taus complex (ZTT). In its SW part it intersects an important mylonite zone with the embedded "Bavarian Pfahl".

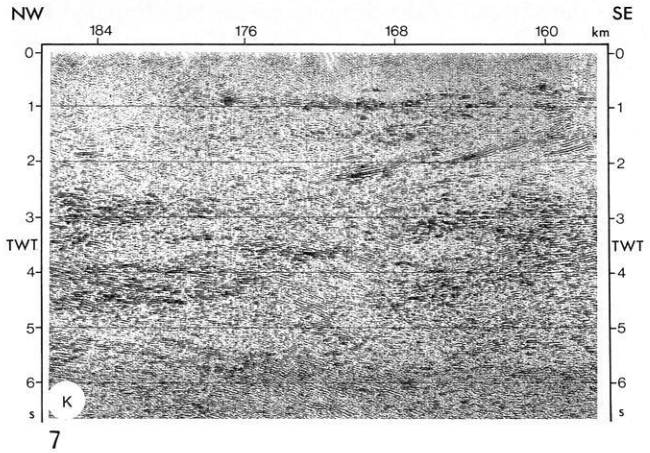

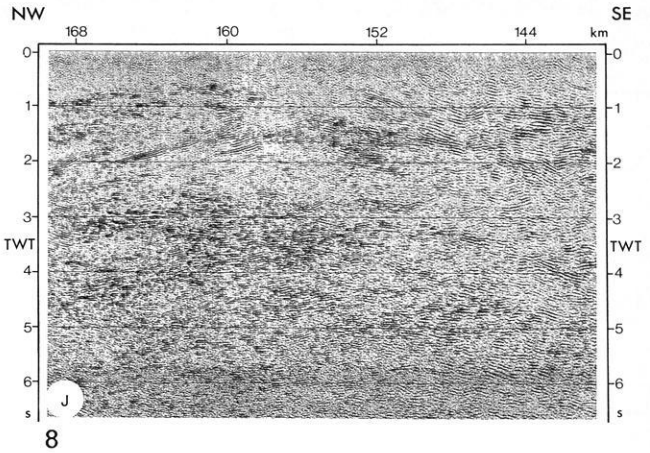

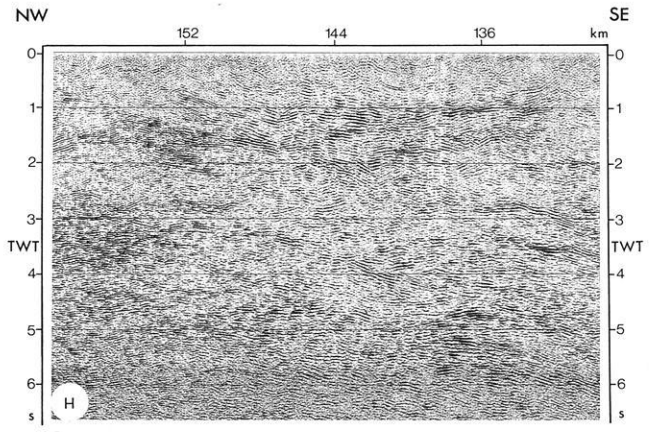

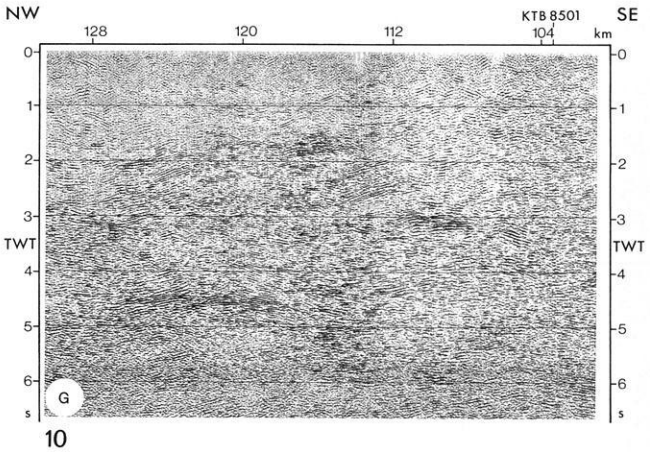

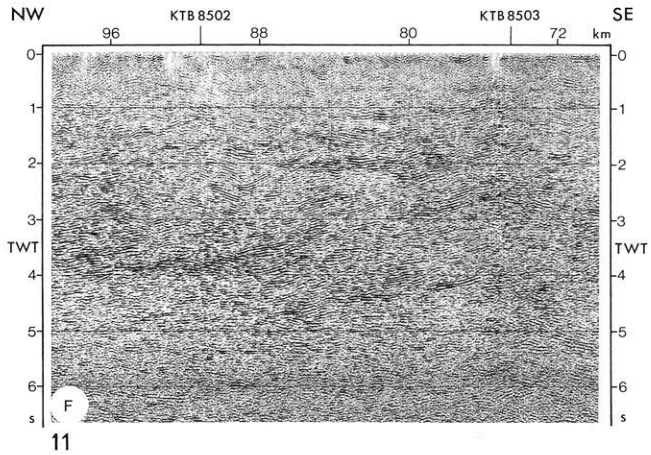

Figs. 7–11. Profiles DEKORP 4; parts of migrated section (see Fig. 6)

The seismic section shows only a few strong events. One of the most prominent results on this profile is a steeply NE-dipping reflection band (true dip angle, about 43°) to be observed over more than 10 km from 0.5–2.5 s TWT, which is to be correlated somehow to the "Pfahl" and its associated mylonites (Fig. 5) outcropping at the surface just at the linear extrapolation of the reflecting band. The event cannot be interpreted as a reflected refraction because the observed, corresponding refractor velocity would be 8.0 km/s and, therefore, is much too high. Moreover, no corresponding refractor is observed in this area and the possibility of side reflections can be excluded by the information from DEKORP 4. Perhaps the NE-dipping reflections with the same steep angle at 5.5–6.0 s TWT further to the NE may be connected to this reflection band, revealing a very great depth range of the "Pfahl".

The horizontal band of reflections at the NE end of 4 Q at 3 s TWT corresponds to likewise horizontal reflections on DEKORP 4 at the intersection of 4 and 4 Q. The corresponding horizon, therefore, has no essential dip and may be related to a deeper thrust plane. At about 7.5–8.0 s TWT a band of strong reflections forming a slight antiformal structure is recorded in the centre of the profile. This band corresponds to the SE-dipping reflectors observed along the SE part of DEKORP 4.

Reflections from the Moho cannot be found on this line. The Moho is probably too deep compared with the recorded reflection time of 12 s.

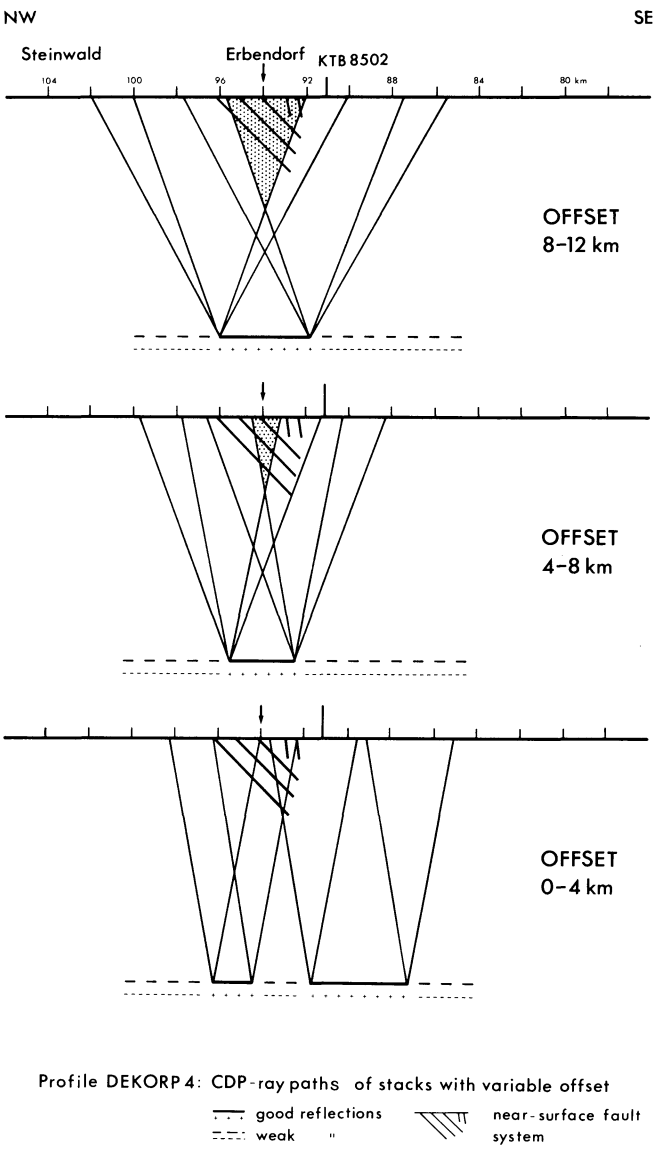

Fig. 12. Profile DEKORP 4: CDP ray paths for stacks with restricted offsets corresponding to Fig. 3

3.2 Lines KTB 8501–8506

KTB 8501

Profile KTB 8501 is the northernmost of the three lines running NE/SW, parallel to the Variscan strike 10–12 km north of the KTB borehole. Some of the features can be followed through all these lines. The line-drawing of KTB 8501 is given in Fig. 18.

At the SW end subhorizontal reflections occur, near the surface, corresponding to sedimentary structures west of the Franconian Line (FL). At this important tectonic lineament the reflections are cut off abruptly. The base of the Permo-Carboniferous is situated at about 0.5 s TWT, corresponding to approximately 1 km depth.

Steeply NE-dipping reflections appear on the NE side of the FL which should derive from a fault plane; they approach a band of strong subhorizontal reflections at about 3 s TWT. This band is related to the reflections originating from the base of the EB as observed in lines KTB 8505 and 8506.

At the SW end of the section another NE-dipping band of reflections appears at 3–5 s TWT. It cannot be interpreted as reflected refractions, but must be real reflections.

The Moho is represented by weak, but continuous, reflections at about 10.5 s TWT.

KTB 8502

Figure 19 shows the migrated section and Fig. 20 the line-drawing of KTB 8502. The sedimentary structures west of the FL are well depicted; they are dragged upwards and cut off abruptly by the crystalline rocks east of the FL. The base of the sediments is situated at 1.2 s TWT, corresponding to about 2.1 km depth.

Below the sediments, strong reflections come from within the crystalline basement showing a pronounced synformal structure. This feature is paralleled by an extended group of exceptionally strong reflections covering the range from 2–5 s TWT at the SW end of the profile with NE dip (Fig. 21). At their NE end one might see a narrow zone void of reflections, which could be interpreted as the subvertical continuation of the FL to depth.

Northeast of the FL, subhorizontal reflections at a level between about 2 and 4 s TWT are observed belonging to the top and base of the EB. They are intersected by several NE-dipping thrust faults along which the EB has been upthrown stepwise to the NE. An attempt to correlate the strong reflectors of the upper crust results almost necessarily in the construction of various steep-angle faults NE of the FL.

At the NE end of KTB 8502 the whole crust is highly reflective from about 2.5 s TWT down to the Moho range at about 11.0 s TWT. The Moho rises toward the SW to about 10.0 s TWT, exhibiting a slight antiform in the centre of the profile.

KTB 8503

Also on this line (see line-drawing in Fig. 22) the sediments west of the FL are represented by strong reflections reaching down to about 1.5 s TWT (approx. 2.9 km depth).

As on line KTB 8502 NE of the FL, NE-dipping reflections cross a broad band of subhorizontal reflections between 2.5 and 4.0 s TWT. These subhorizontal reflections are related to the EB. At the SW end of the section, again, strong synformal reflections appear at 2.5–4.0 s TWT. Their structure parallels the base of the Permo-Carboniferous, but they are certainly not multiples.

The Moho is represented by an antiformal band of reflections between 9.5 and 11.0 s TWT indicating an anticline in the centre of the profile, similar to that on profile KTB 8502.

KTB 8504

On line KTB 8504 (Fig. 23) the strongly structured morphology of the sedimentary trough west of the FL is apparent. Its basement is related to the base of the Permo-Carboniferous and shows two pronounced highs in the northern half of the profile and a remarkable depression in the SE at about 1.8 s TWT, corresponding to approximately 3 km depth.

At the NW end of the section strong reflectors appear at 2.0–2.5 s TWT, dipping SE. Their structure has no rela-

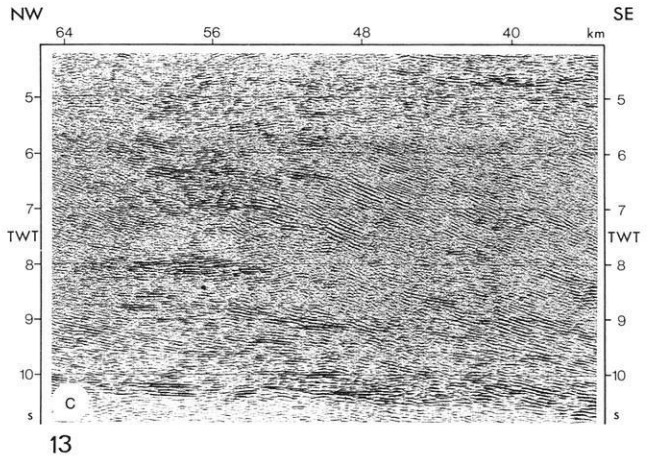

13

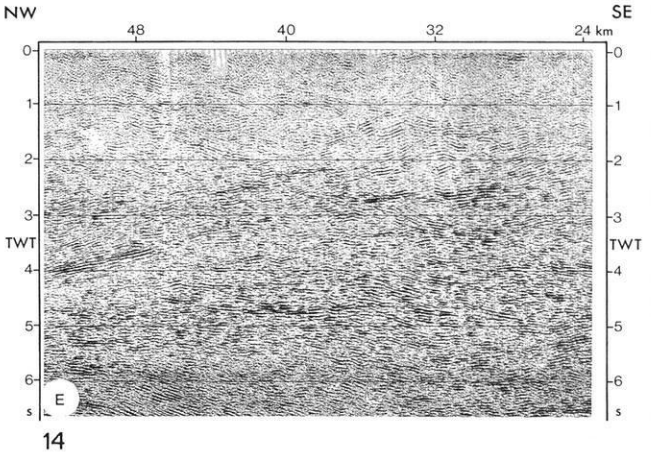

14

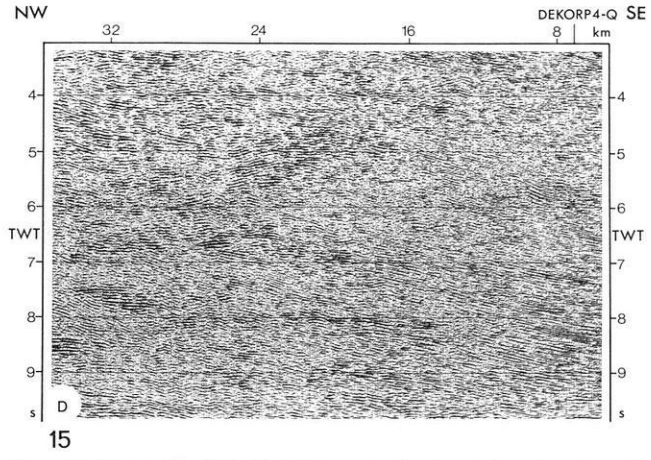

15

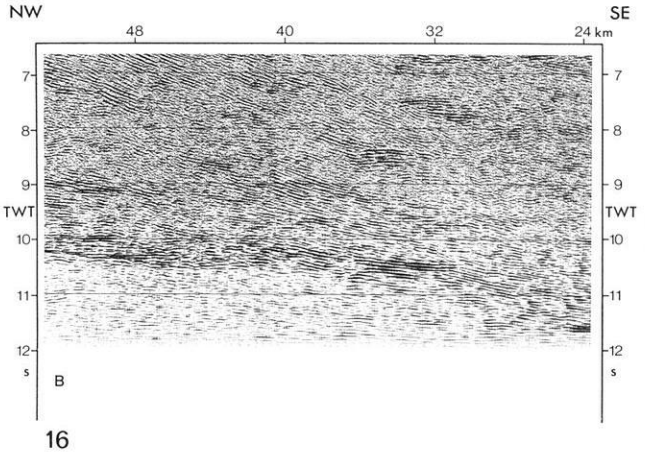

16

Figs. 13–16. Profile DEKORP 4; part of migrated section (see Fig. 6)

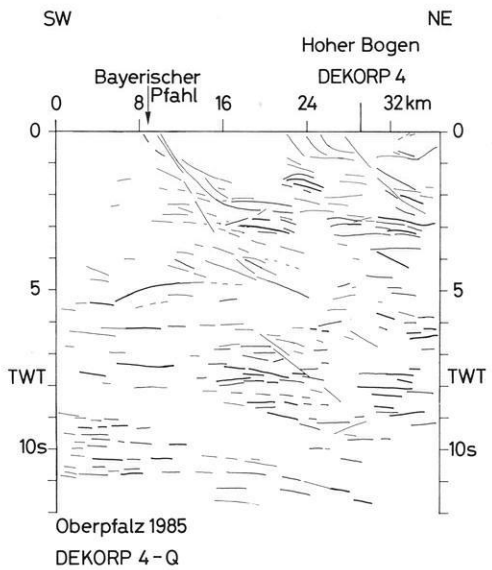

Fig. 17. Profile DEKORP 4-Q; line-drawing of the migrated section

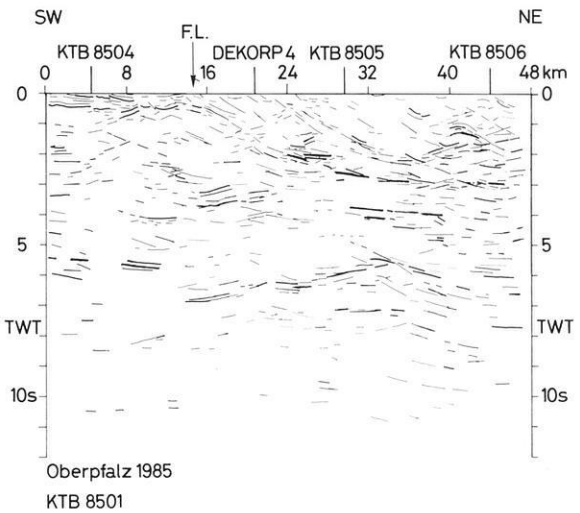

Fig. 18. Profile KTB 8501; line-drawing of the migrated section

tion to the base of the sediments. In the SE half of the profile below the sedimentary basement, another sharply pronounced synformal structure is observed approaching the basement at the intersection with line KTB 8502 and reaching its maximum depth at about 3.5 s TWT. A broad band of reflections follows from 3.5–5.0 s TWT, extending from the SE end of the profile to about its centre. It might correspond to the SW extension of the EB, but this is mere speculation at this stage of the investigation. The range below is nearly void of reflections except for a small part at the utmost SE end between 9 and 10 s TWT, corresponding to the Moho level.

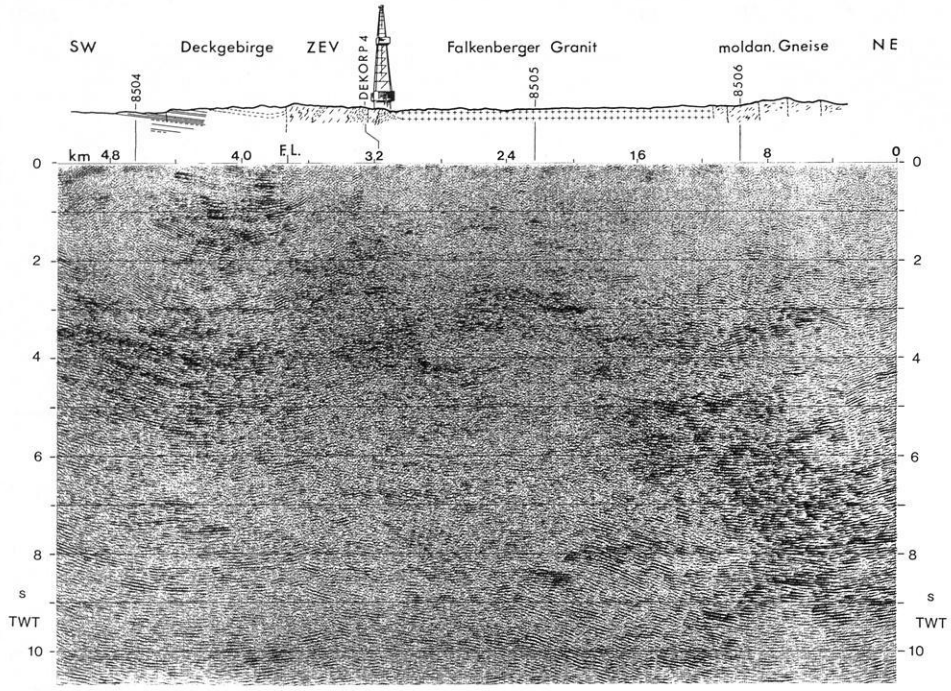

Fig. 19. Profile KTB 8502; migrated section

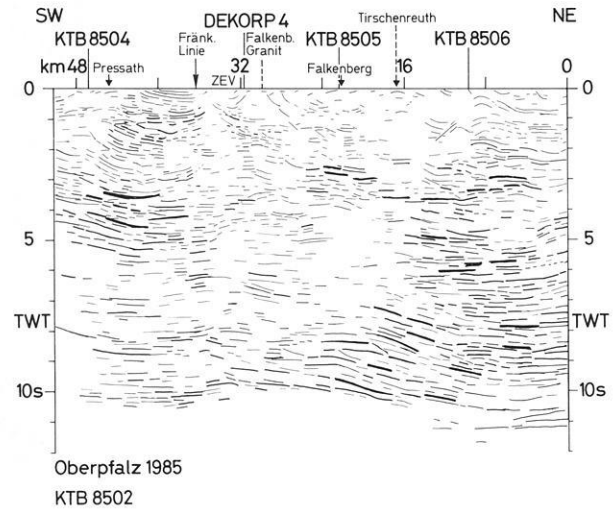

Fig. 20. Profile KTB 8502; line-drawing of the migrated section

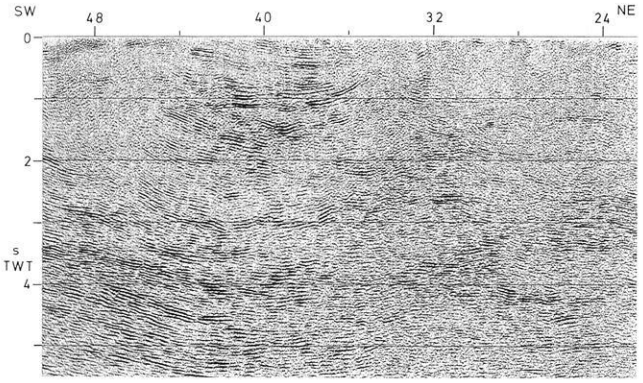

Fig. 21. Part of profile KTB 8502; migrated section

KTB 8505

Profile KTB 8505 (see line-drawing in Fig. 24) is characterized by SE-dipping events crossing the entire crust. In the SE part a pronounced rhombic structure with an internal imbrication ("Schuppenkörper") is observed at 2.5–4.0 s TWT, passing over into a subhorizontal strong reflector (Fig. 25). This pattern is related to the EB observed on line DEKORP 4 at a somewhat deeper level but with a similarly remarkable shape.

Beneath the EB – contrary to the observation on DEKORP 4 – a great number of SE-dipping and subhorizontal reflections show up over the range from 4.0 to 10.5 s TWT.

The Moho is represented by a flat band of reflections between 9.5 and 10.5 s TWT.

Generally, the seismic pattern is in close accordance with the structures found on line DEKORP 4, exhibiting the steeply SE-dipping structures and the wedge-like shape of the EB as well.

KTB 8506

This line (line-drawing Fig. 26) differs from the other cross-strike profiles in showing a pronounced and nearly continuous SE dip all along the line.

Many SE-dipping reflections of great strength can be observed coherently over a long distance, crossing the crust from the uppermost to the lowermost parts. In the near-surface range, SE-bending events correspond to listric fault planes (Fig. 27).

Again, in the SE part of the profile a strong imbricated structure appears between 2.5 and 4.5 s TWT, overriding the SE-dipping band of reflections (Fig. 28). The reflection seismic correlation of these features along the network of seismic lines implies that this "Schuppenkörper" is also part of the EB. Thus, a lateral extension of this body in the Variscan direction, of at least 32 km, can be derived.

In contrast to the other two parallel lines, the Moho is only poorly recognizable. It is suspected at about 10.5–11.0 s TWT, corresponding to 31.5–33.0 km depth.

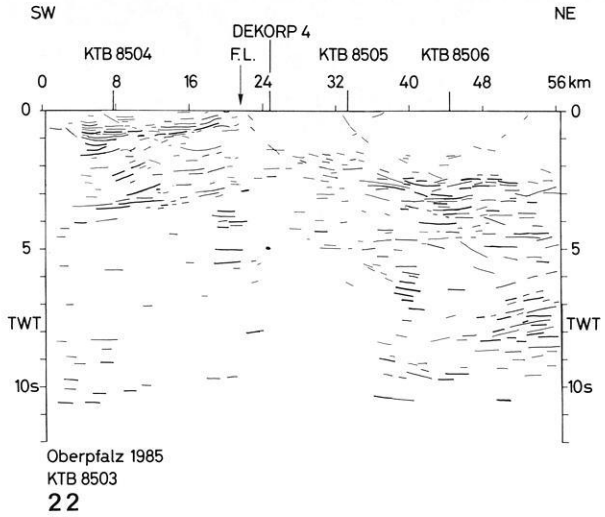

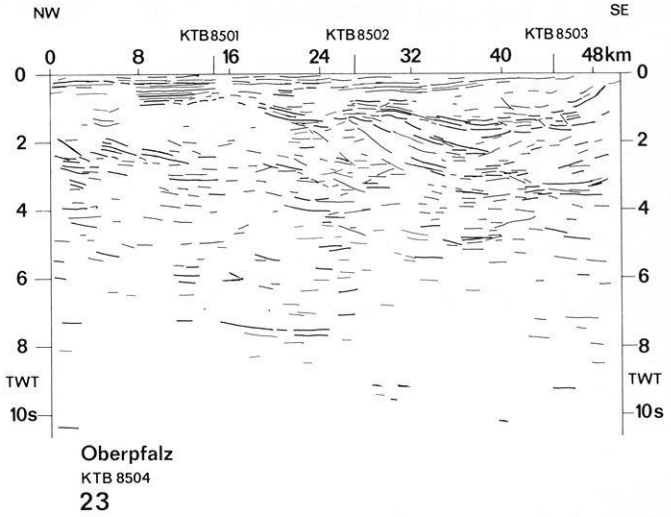

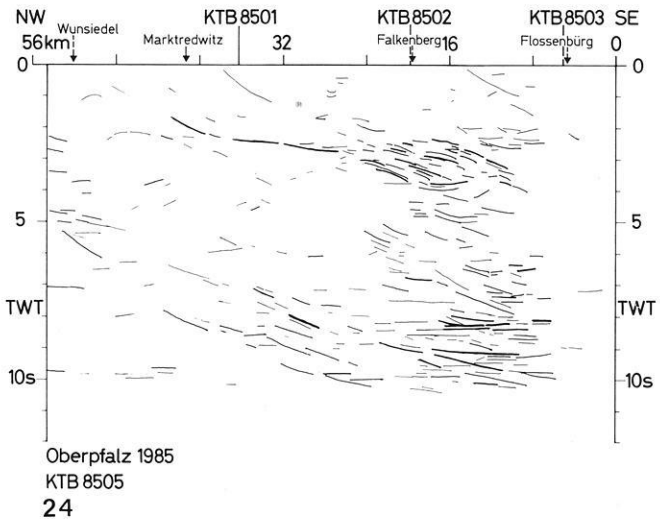

Fig. 22. Profile KTB 8503; line-drawing of the migrated section

Fig. 23. Profile KTB 8504; line-drawing of the migrated section

Fig. 24. Profile KTB 8505; line-drawing of the migrated section

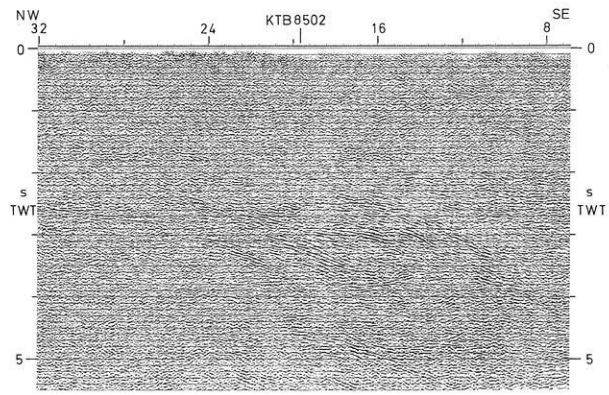

Fig. 25. Profile KTB 8505; part of migrated section with the Erbendorf body

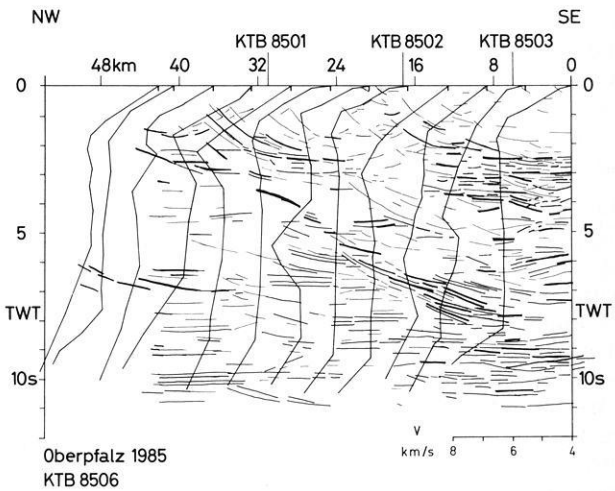

Fig. 26. Profile KTB 8506; line-drawing of the migrated section with interval velocities from DMO-processed stacking velocities

The line-drawing of Fig. 26 simultaneously presents the velocity-depth functions for profile KTB 8506 which have been derived from the DMO processing and which can be regarded as more reliable than velocity information derived from other routine processing techniques applied to deep reflection seismic data (cf. Section 2.2). The resulting velocity distribution is essentially similar to that obtained by wide-angle data along the parallel DEKORP 4 profile (Section 4).

Figure 29 shows an arrangement of line-drawings with the most important reflection elements of the parallel lines DEKORP 4, KTB 8505 and KTB 8506. The EB is indicated

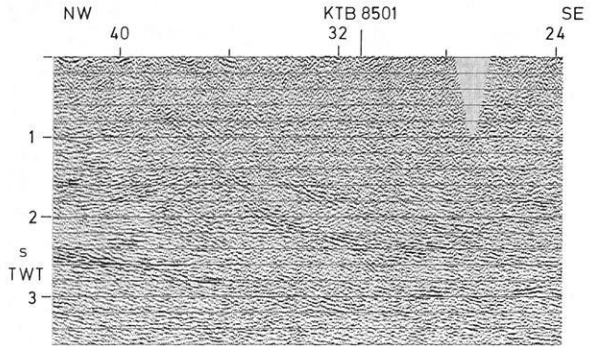

Fig. 27. Profile KTB 8506; part of migrated section with listric shear planes

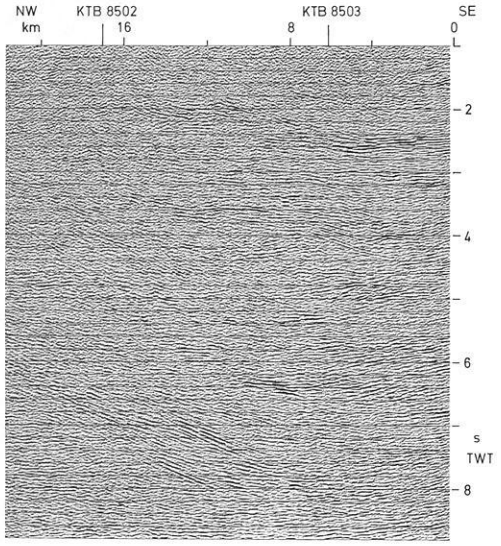

Fig. 28. Profile KTB 8506; part of migrated section with Erbendorf body and dipping reflections in the upper and lower crust

by the shaded area. Its size and extension on the three cross-strike lines and the dominance of the SE-dipping elements is clearly defined.

Results from first arrivals and shot-hole logging

Geological shot-hole logs served to complement general geological information when setting up the geological section along the centre part of profile DEKORP 4. Refractor velocities derived from first arrivals agree qualitatively with major lithologies as found in shot holes. The ZEV may serve as an example (Fig. 30). Here, refractor velocities above 6000 m/s confirm the massive occurrence of amphibolite in the northern half of the ZEV, whereas velocities in the diaphthoritic shear zone at its southern margin drop sharply to less than 4500 m/s. Within the Hoher Bogen complex at the southern end of DEKORP 4, refractor velocities may even reflect different amphibolite varieties. The rise of a refractor with 6300 m/s to less than 50 m below the surface seems to confirm a narrow zone of suspected eclogites and/or ultramafics within the "Gabbroic Amphibolite" (Fig. 31). Schistose fine-grained amphibolites (GAm) of presumably lower bulk density and larger V_p anisotropy (Christensen, 1965) show consistently lower refractor velocities than the coarse-grained amphibolites (Gb).

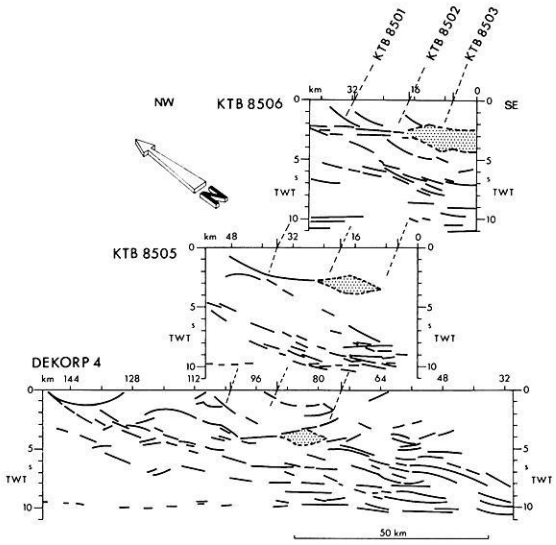

Fig. 29. Arrangement of line-drawings with the prominent elements of lines DEKORP 4, KTB 8505 and 8506. *Hatched* – Erbendorf body

One-dimensional velocity models from first arrivals on profiles KTB 8501–8504 were used to infer depths to the pre-Permian basement in the foreland basin SW of the FL. The modelling was hampered by the seismic spread being too short relative to the depth of the pre-Permian unconformity in the southern half of KTB 8504. This problem was partially overcome by additional observations of first arrivals from vibrator points at larger offsets. Reflection times calculated from the refraction data fit the reflection pattern fairly well so that the computed depth of the basement is believed to be correct within 10%. At the SW end of profile KTB 8503 the results are in agreement with a depth contour map of the basement derived from a number of wells (Helmkampf et al., 1982).

The results are shown in a block diagram (Fig. 32). They indicate high relief of the floor of the Permian basin, with troughs and highs probably extending parallel to the older Variscan trends. Permo-Carboniferous basin fill may reach 2.5 km in the Weiden area. These findings are in general agreement with earlier gravimetric models (Fuchs and Soffel, 1981). The relief was buried at the end of the Permian so that Triassic and probably Jurassic strata blanketed all earlier structures SW of the FL (Leitz and Schroeder, 1985). Post-Jurassic sedimentation and inversion produced shallow synclines and anticlines trending roughly NW/SE. They show up clearly in the reflector pattern: a brachyanticline on profile KTB 8501, a syncline with remnants of Upper Cretaceous on KTB 8502 and a part of the Kaltenbrunn antiform (Leitz and Schroeder, 1985) on KTB 8504 close to the intersection with KTB 8503. Only on profiles KTB 8501 and 8503 does the post-Cretaceous inversion seem to have appreciably overprinted the older basement topography by high-angle faults, apparently supporting contraction subperpendicular to the foreland basin axis.

3.3 Depth contour maps

Figure 33 shows the map of the base of the EB using the previously indicated correlation. For depth inversion, a mean crustal velocity of 6.0 km/s was assumed (see Section 4.2). Northwest of the dashed line, indicating the boundary

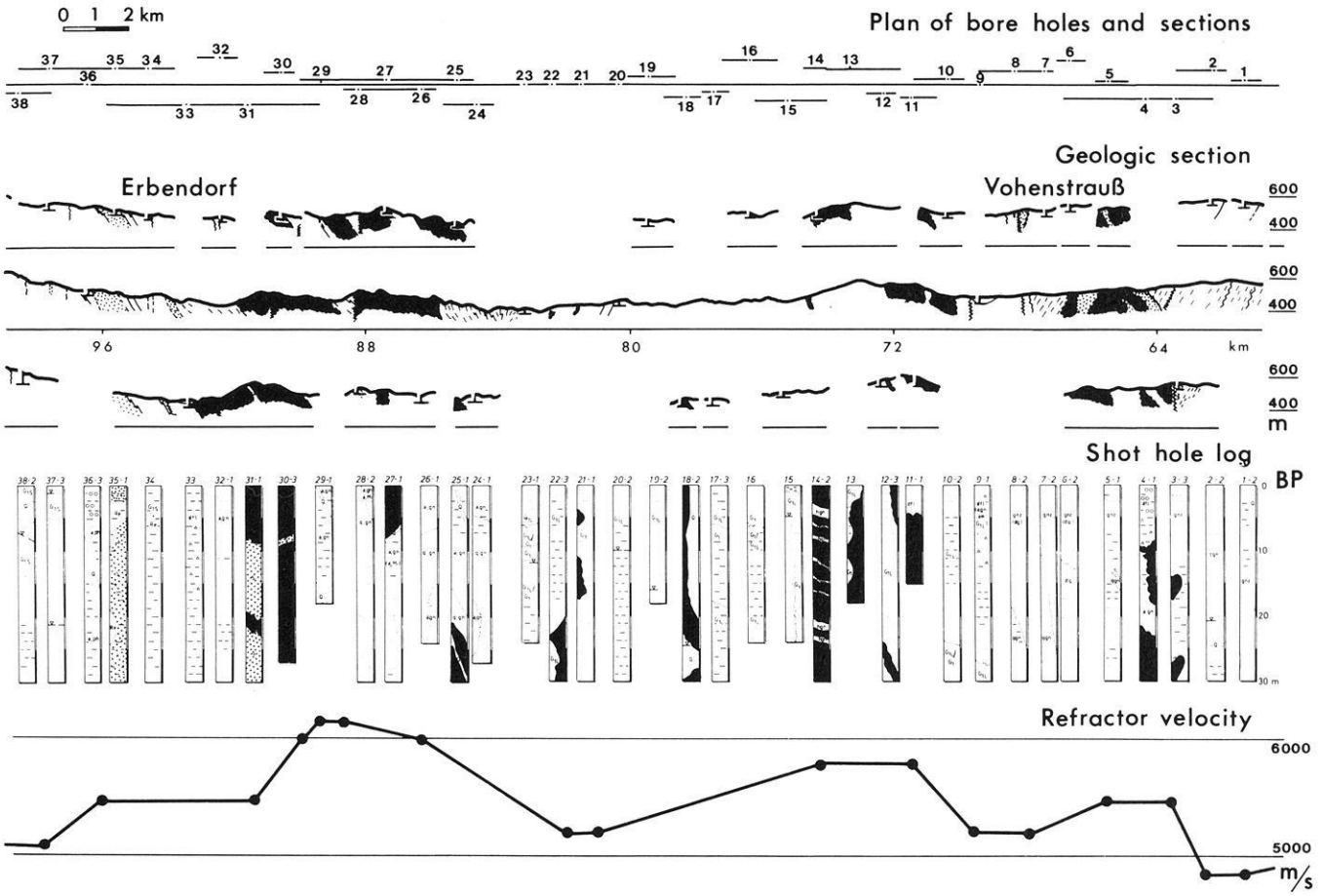

Fig. 30. Correlation of lithology and refractor velocity in the ZEV segment of DEKORP 4; *black* = amphibolite, *dots* = serpentinite, *dashes* = gneiss, *blank* = granite

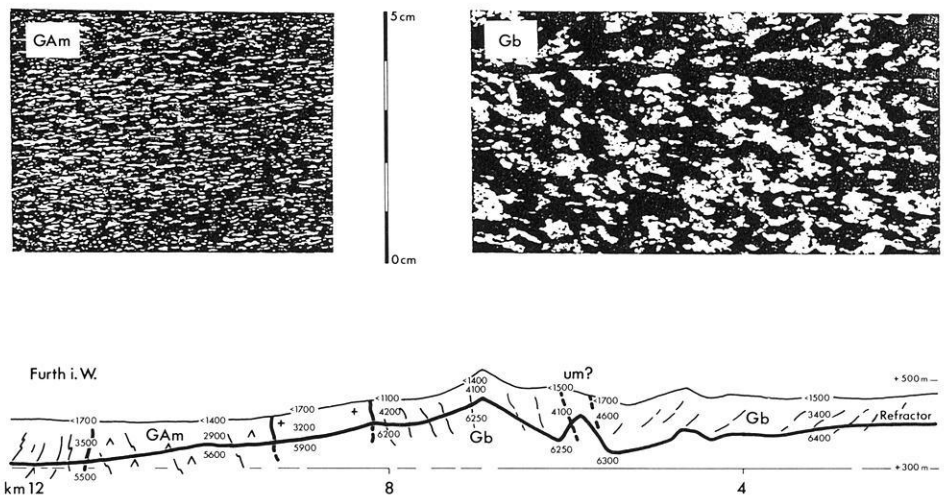

Fig. 31. DEKORP 4, southern end (Hoher Bogen amphibolite complex). *Top*: characteristic textures of amphibolites; *bottom*: geological section and velocities from first arrivals. Note: refractor velocities near 5600 m/s correspond to schistose amphibolite (GAm) of Hoher Bogen complex, velocities around 6200 m/s reflect gabbroic amphibolite (Gb); *um* = suspected ultramafics

of the EB, the mapped horizon represents the possible "master décollement". The character of the reflections in the corresponding parts of the profiles is due to uncertainties: in the NW part of KTB 8506 two different décollement planes seem to be present, differing in depth by about 2.5 km. The depth of the shallower plane is indicated by numbers in square brackets.

In this interpretation the mapped horizon is intersected by several NW- to SE-striking reverse faults. Generally, the horizon dips from NW to SE; on line DEKORP 4 its highest position is north of the intersection with KTB 8501 and another maximum occurs between KTB 8501 and 8502 near the drilling location.

The question of whether the EB continues west of the FL cannot be answered with the present data. However, at the appropriate depth range, good reflecting horizons occur. Their structural position is indicated by the symbols for a synform axis. This axis runs between KTB 8501 and

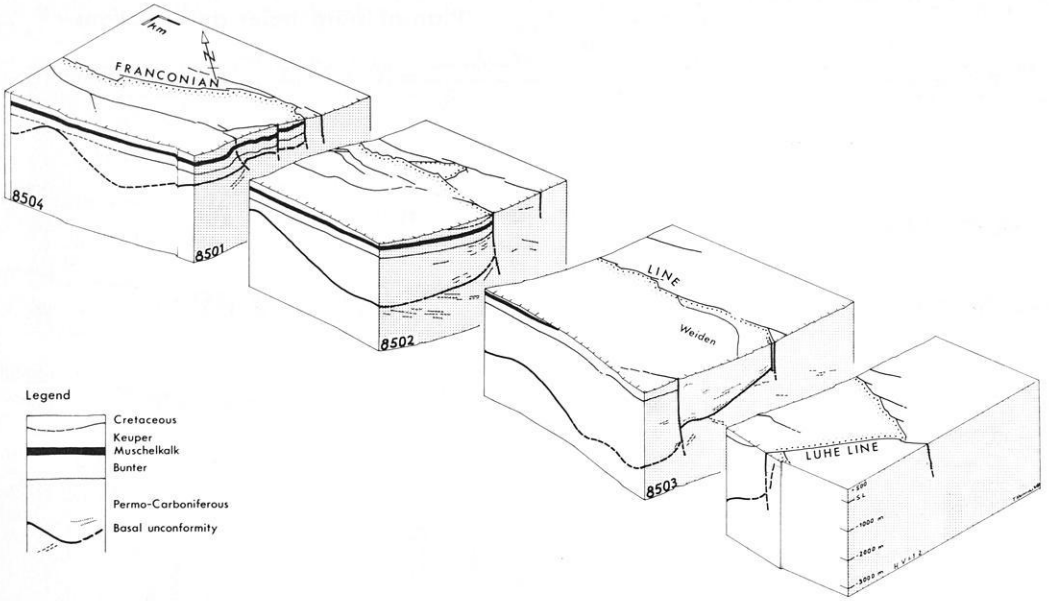

Fig. 32. Block diagram of Permo-Mesozoic foreland basin SW of Franconian Line. Mesozoic structure constrained by depth contour maps and boreholes Wollau and Parkstein (Haunschild and Schröder, 1960; Schröder and Siegling, 1966; Gudden and Schmid, 1985; Emmert, 1981)

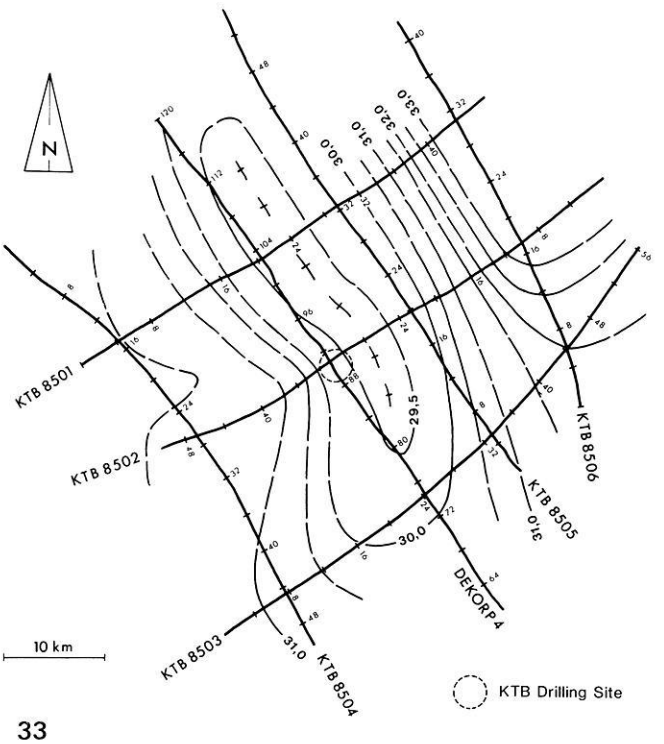

33

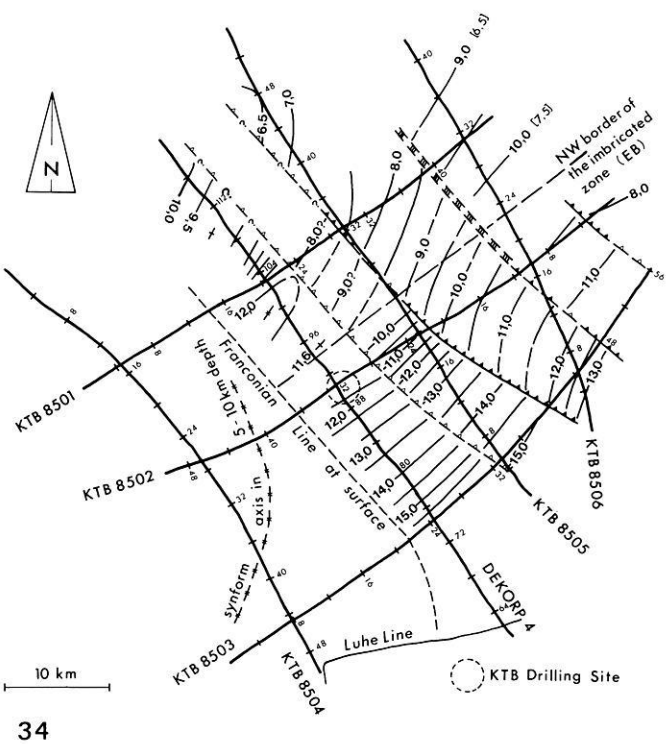

34

Fig. 33. Depth contour map of the Erbendorf body base and the corresponding décollement plane (depth in km, $V_{average} = 6$ km/s)

Fig. 34. Depth contour map of the Moho (depth in km, $V_{average} = 6$ km/s)

8502 in a NW/SE direction, changing, however, north of KTB 8503 (NW of the Luhe Line) into a SW direction.

Figure 34 shows an attempt at a depth contour map of the Moho, again using a mean crustal velocity of 6.0 km/s. The dominating NW- to SE-striking anticlinal axis is based essentially on KTB 8502. Along the remaining profiles, speculative supplements were partly necessary. In the area of the drilling location the Moho presents a high with its axis striking NW/SE and changing north of the Luhe Line into a S-to-SW (?) direction similar to the syncline axis of Fig. 33.

At the intersection of profiles DEKORP 4 and KTB 8502, i.e. close to the location of the KTB borehole, the true position in space and the true dip have been computed for such reflecting elements whose components of dip could be determined along both profiles (Fig. 35). There are two main azimuths of tectonic directions; NW/SE and SW/NE. The elements dipping NE probably derive from several

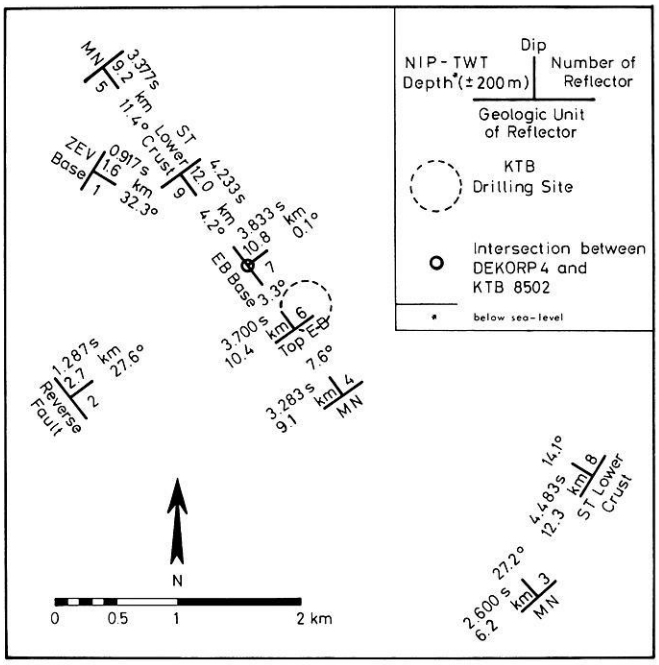

Fig. 35. True incidence and true position of the common reflection points of the intersecting lines DEKORP 4 and KTB 8502

faults, and not from lithological boundaries. A detailed discussion on these elements is given in Section 5.

4 Accompanying seismic surveys and their first results

4.1 Field techniques

In addition to the Vibroseis near-vertical reflection survey, a series of 96 borehole shots with charges of 90 kg and 1-km spacing was fired in the north-western part of the DEKORP 4 line. These shots were used for three different supplementary programs:

1. For mapping wide-angle reflections from the upper crust by means of the contractor's 200-channel reflection spread operated at 42–58 km offset
2. For mapping lower-crustal and Moho wide-angle reflections with a mobile array of 24 3-channel MARS stations at 60–90 km offset
3. For two expanding spread experiments with midpoints in the Moldanubian and Saxothuringian zones

The observational scheme is shown in Fig. 36. Shots moved 4 km/day from shotpoint 1 near Vohenstrauß towards the northwest, while the contractor's spread and the MARS array (operated by university teams from Berlin, Clausthal, Frankfurt and München) followed at constant mean shot-to-receiver offset. The expanding spread equipment with a total of 120 channels from the universities of Clausthal, Hamburg and Kiel, and from BGR/NLfB Hannover, moved with the same velocity in the opposite direction to keep common midpoints stationary.

The shots were fired in the late afternoons, after the daily Vibroseis work. With some exceptions, especially in dry and hard rocks, their seismic efficiency was sufficient and the noise level at the recording sites was low enough to yield good seismograms up to maximum distances of 100 km.

4.2 Results of the wide-angle reflection survey

Figure 37 shows a detailed location map of the shotpoints and the MARS stations. The shot-to-receiver midpoints are plotted in Fig. 38. They cover 100 km of the DEKORP 4 line and cross the tectonometamorphic boundary between the Saxothuringian and the Moldanubian units of the Var-

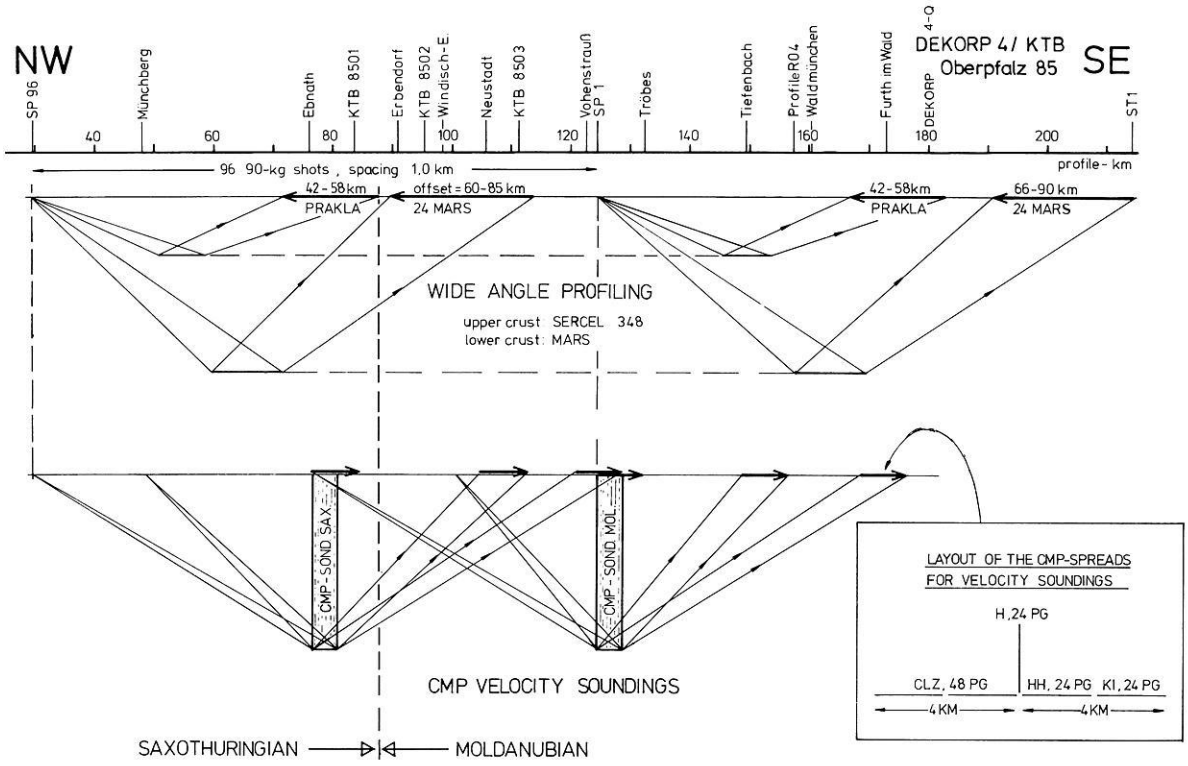

Fig. 36. Observational scheme of the wide-angle seismics, Oberpfalz 1985

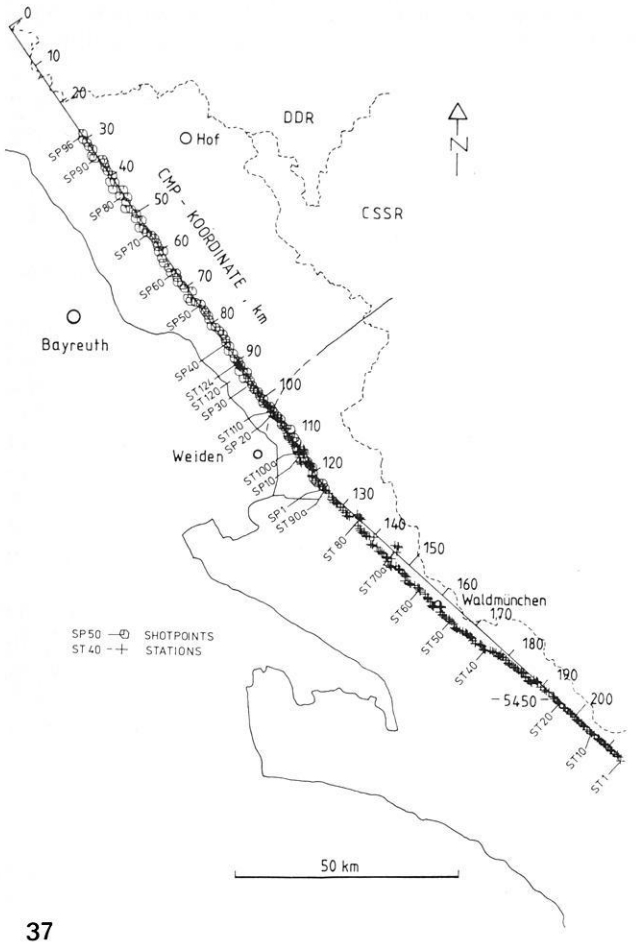

37

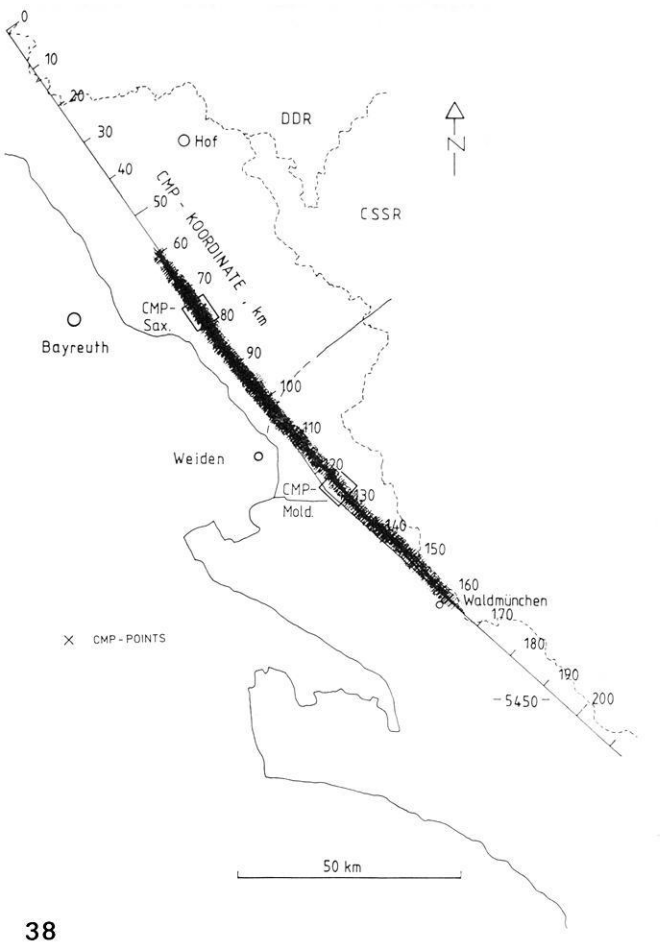

38

Fig. 37. Location map of the shotpoints and MARS stations for the wide-angle mapping along DEKORP 4

Fig. 38. Location map of the shot-to-receiver midpoints (CMP) for the MARS wide-angle mapping. The CMP points for the velocity soundings (Section 4.3) are situated in the *rectangular areas* with centres at profile km 76 and 126

iscides. The CMPs of the expanding spread observations are indicated by open squares in Fig. 38. CMP locations are characterized in this section by a linear southeasterly increasing CMP coordinate, the origin of which is the northwestern end of the DEKORP 4 reflection line.

Due to the multiple coverage, the wide-angle reflections can be processed and presented in different ways. In the following, particular use is made of the common-midpoint (CMP) and common-offset (COF) sorting possibilities. CMP sorting suppresses the influence of dip and is therefore particularly suitable for velocity analysis, whereas COF sorting is particularly suitable for structural imaging.

Indications showing an unusual distribution of seismic wave velocities in the investigated area had already been obtained from regional refraction seismic surveys (KTB, 1986, p. 113). Wide-angle mapping combined with DEKORP 4 should serve to investigate this phenomenon, both in detail and in the regional context. A small part of the comprehensive observation material is given in Figs. 39 and 41–43 for the constant-shotpoint (CSP) and COF configurations.

Figure 39 shows three single shot observations in the 42–58 km distance range with predominant wave propagation in the ST, in the ST/MN boundary domain and in the MN. Structural changes become obvious along the DEKORP 4 line, which with examination of the CMP sections in Fig. 41 a and b becomes even clearer. Immediately after the P_g first arrivals, which were clearly observed over about 60 km both in the ST and the MN with apparent velocities of about 6 km/s, complicated wave groups follow which cannot be individually resolved using the wide-angle seismics method but which must be interpreted as indications of a small-scale heterogeneous structure of the upper crust. The boundary domain between profile km 80 and 110 (Neusorg-Weiden) deviates from this by two important features:

1. The first arrivals terminate at a distance of 40–50 km, which implies a relatively shallow position of a low-velocity zone (LVZ) in the upper crust.

2. In the distance range of 40–70 km with reduced travel times of 1.5–0.5 s, an unusually intensive and well-correlatable wide-angle reflection appears (in Fig. 39, centre, indicated by P_EP), with apparent velocities up to 8 km/s.

This prominent wide-angle reflection, that had already been found during regional surveys by means of quarry blasts, is caused by a crustal domain at a depth of 8–13 km, the Erbendorf body (EB), that is also characterized in near-vertical angle seismics by an unusually high reflectivity (Figs. 6 and 11). Its NW/SE extension is best recognized in the CMP sections (Fig. 41 a and b) and the COF sections

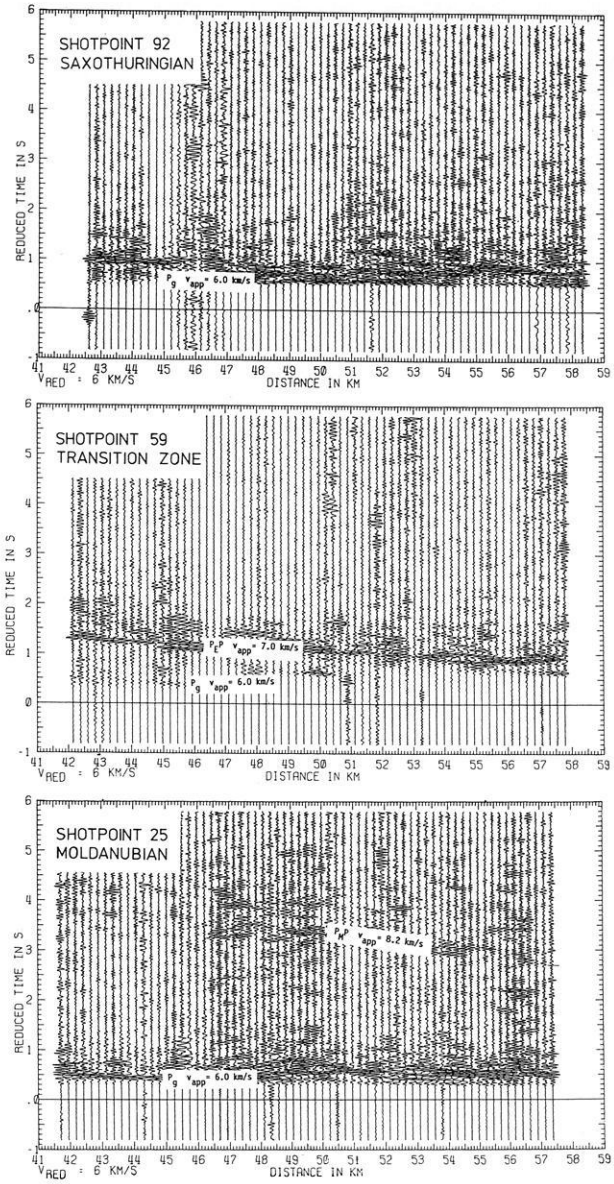

Fig. 39. Single-shot playbacks for the ST (SP 92, *top*), the MN (SP 25, *bottom*) and the boundary domain between them (SP 59, *centre*), reduced by 6 km/s. In the ST and in the MN, clear P_g first arrivals with apparent velocities of approx. 6.0 km/s can be observed in the distance range shown, followed by complicated, non-resolvable wave groups. In the boundary domain, the P_g first arrivals terminate at about 46 km and, with a clear gap in time, are followed by a pronounced wide-angle reflection P_EP with apparent velocities of about 7.0 km/s

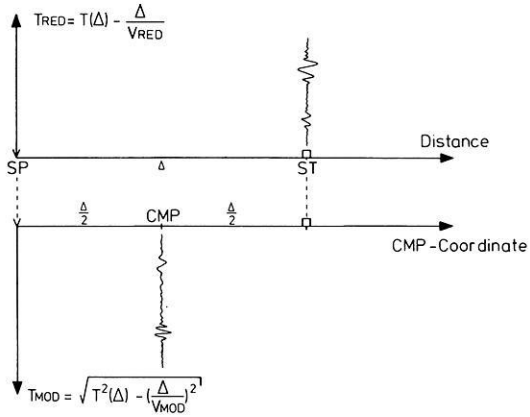

Fig. 40. Comments on the principle of presenting CMP and COF wide-angle sections: With common-shotpoint or common-receiver point sections the seismograms are usually plotted against the observation distance (offset) with reduced time T_{red} in the upward direction. CMP sections are represented in the same way, except that these are seismograms for shotpoints and receiver points with a common midpoint (CMP). On the other hand, in COF sections seismograms for source-receiver pairs with equal offset (*c*onstant *o*ffset) are plotted against the centre-point coordinates with modified time T_{mod} in the downward direction

(Fig. 42a and b). Figure 41a and b gives a selection of 6 sections from a total of 46 CMP sections, in which that part of the profile between 60 and 150 km is covered at 2 km intervals (Fig. 37). The wide-angle image of the EB appears most clearly at CMP points 86–96; Fig. 41a, bottom, shows a typical example. CMP 84 (Fig. 41a, centre) and CMP 98 (Fig. 41b, top) indicate the margins beyond which the EB cannot be traced by wide-angle seismics.

Clear P_iP reflections originate from the deeper crust at km 92 as separate phase groups (in Fig. 41b, centre, with reduced travel times between 2 and 3s) and approaching the MN, Moho reflections (P_MP) occur more frequently. Between 102 and 106 km, the latter are characterized by apparent velocities up to 10 km/s even in the dip-insensitive CMP sections, from which (in connection with reversed observations) a SE dip of the Moho up to 10° must be concluded. In the MN proper, the CMP sections show a heterogeneous, but not clearly structured, upper crust, now and then good P_iP reflections from the middle crust (top of the lower crust?) and usually clear Moho reflections (e.g. CMP 130 in Fig. 41b).

Crustal structuring becomes more clearly recognizable in the COF sections (Figs. 42a–c, 43). The construction principle of these constant-offset sections is explained in Fig. 40. Basically, zero-offset sections have been simulated by dynamic correction of COF wide-angle seismograms, corresponding to the dynamic correction of normal seismic reflection data. The near-surface domains cannot be resolved because of the minimum observation distance of 40 km; hence, the time scale for the "modified time" T_{mod}, that corresponds to the two-way travel time in the near-vertical sections begins at 2 s.

Figure 42a shows COF sections for 47 and 53 km offset. In both presentations, which are based on completely independent sets of data, the EB can be recognized as the dominant structure in the upper crust (between profile km 83 and 98 and between 3.5 and 5.0 s modified time). The wide-angle reflections outline an antiformal structure that continues in the NW and SE to deeper crustal levels. Figure 42b shows the EB focussed from other observation distances. The images are not completely identical and also deviate in some detail from the near-vertical reflection seismic image. The reasons are the dependence of reflectivity on the angle of incidence and the unknown detailed velocity structure. The general coincidence underlines the significance of the EB phenomenon.

The middle and lower crust are only inadequately resolved by the small offsets of 47 and 53 km. However, by enlargement of the aperture (COF 72 and 82 km, Fig. 42c), structures at greater depths can also be imaged. It appears that there is a further reflector below the EB with $T_{mod} =$

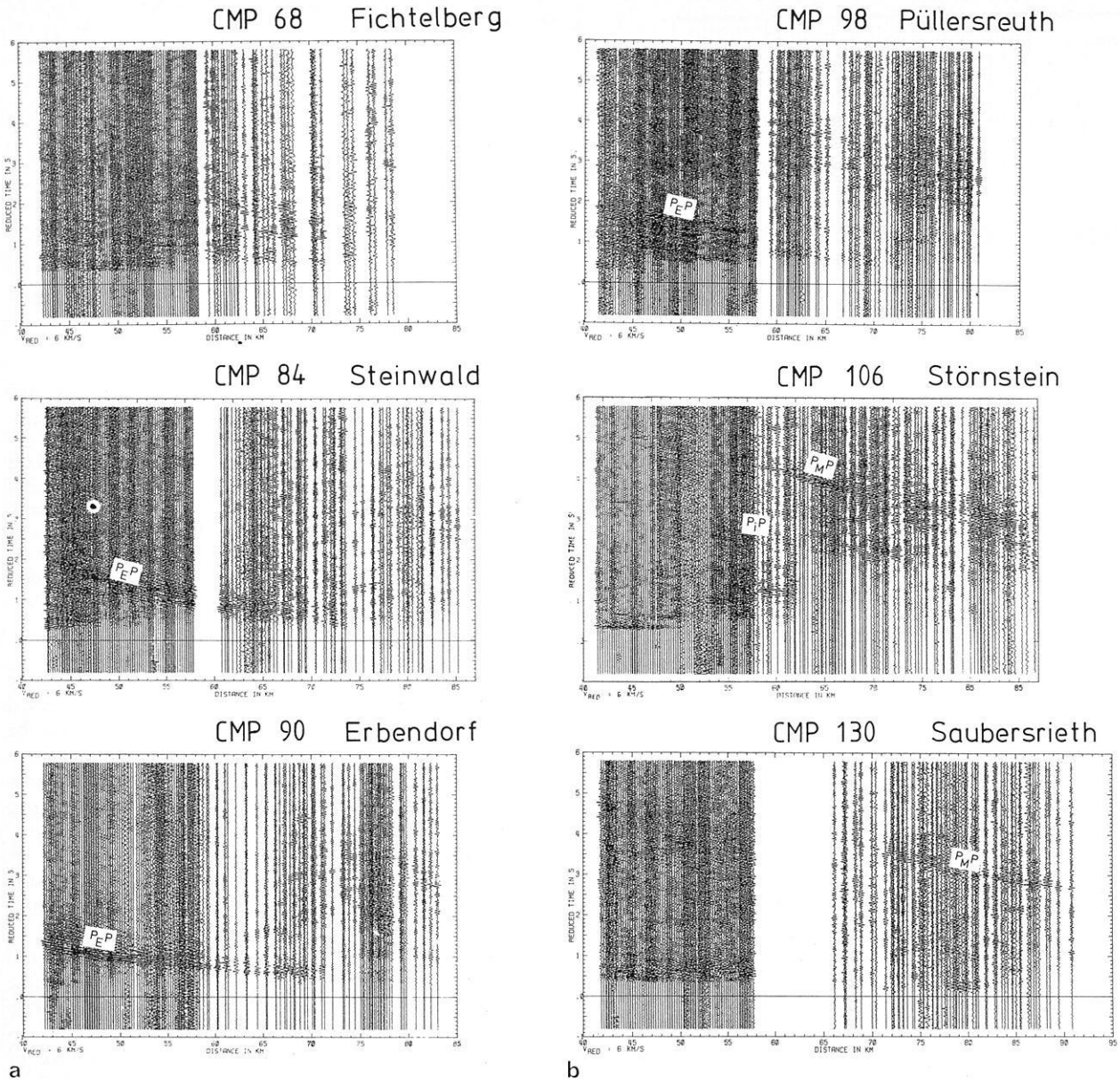

Fig. 41 a and b. Sequence of 6, from a total of 46, CMP sections between the Fichtelgebirge and Oberpfälzer Wald. The CMP gathers shown are derived in each case from an interval of ± 1 km around the given nominal value. CMP 68, Fichtelberg: heterogeneous crustal structure difficult to resolve by wide-angle observations; CMP 84, Steinwald: the EB starts to appear; CMP 90, Erbendorf: clear wide-angle reflection of the EB, high apparent velocities (up to 8.0 km/s) and large amplitudes in the 42–70 km distance range; CMP 98, Püllersreuth: splitting of the EB wide-angle reflection into three diffuse bands; after about 3 s reduced travel time, the typical wide-angle image of the heterogeneous lower crust; CMP 106, Störnstein: LVZ indicated by termination of the P_g branch; relatively clear P_iP reflections from the lower crust; Moho reflection with CMP apparent velocity of 10 km/s indicates Moho dipping to the SE; CMP 130, Saubersrieth: P_g onsets up to 80 km, no clearly structured crust but good Moho reflections

7.0–7.5 s (a depth of approximately 23 km) that presumably marks the top of the lower crust. Accordingly, the EB cannot represent an updoming of the lower crust. If the EB consists of lower-crustal material – both its characteristic reflection behaviour and its velocity advocate this – it must have been brought into its present position by overthrust tectonics (see Section 5).

In Fig. 42c, particularly at COF 82, the Moho is clearly recognized. It rises from the SE towards the NW. However, the rise is not continuous but consists, rather, of small-scale undulations and possible imbrications in the lower crust. Similar structures are imaged by near-vertical seismics (see Fig. 6). A high of the Moho is indicated below the ST/MN boundary domain, but simultaneously the character of the Moho is also more diffuse.

A similar processing of the *S* waves (Bopp, 1986) likewise shows the rise of the Moho from SE to NW and – surprisingly – the Moho high in the ST/MN boundary domain even more clearly than the *P* waves (Fig. 43). On the other hand, it is worth noting that the lower crust, which is clearly imaged by the *P* waves (Fig. 42c), is hardly recognizable in the *S* waves. Sandmeier and Wenzel (1986) have reported similar observations in the Black Forest. This supports the assumption that this could be a general phenomenon of the lower crust.

A first two-dimensional velocity model was established

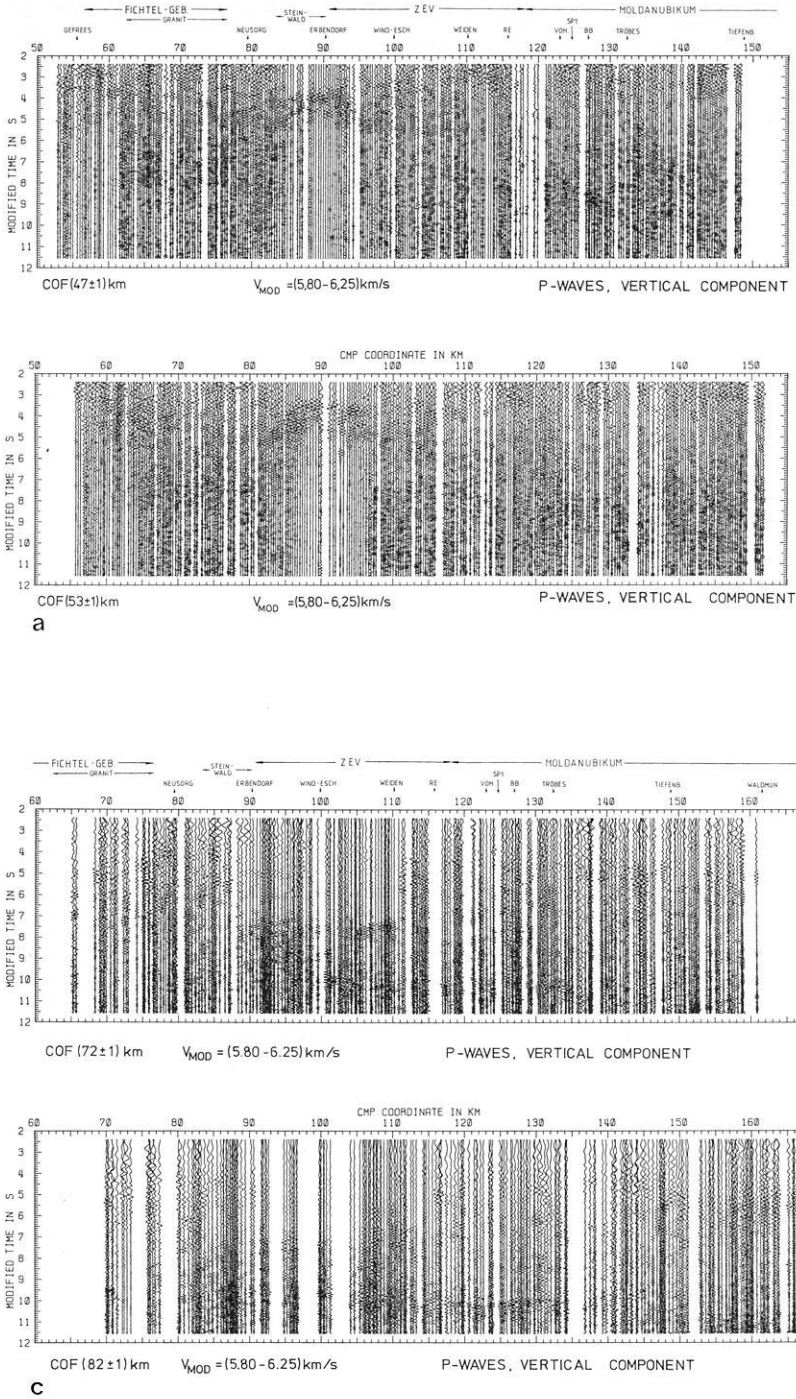

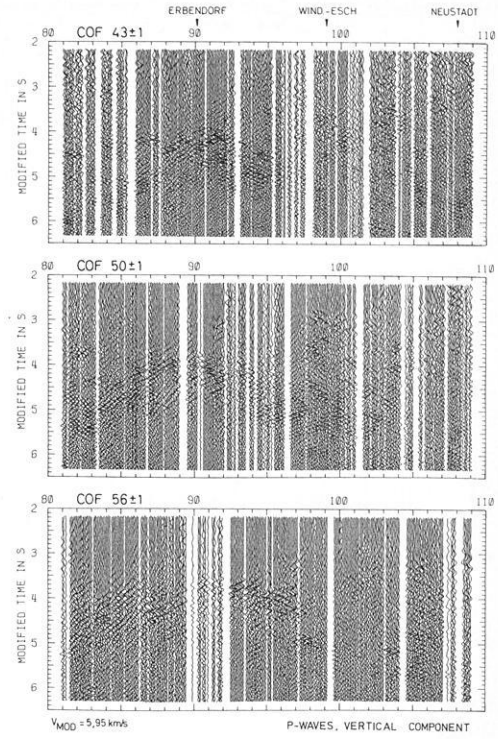

Fig. 42. **a** Dynamically corrected COF sections obtained from observations with the contractor equipment at (47±1) km, *top*, and at (53±1) km, *bottom*. The EB can be recognized as the dominant structure in the form of an updoming with its centre at profile km 90. The *transparent area* below the EB is an artefact of the seismogram normalization with regard to uniform maximum amplitude; in fact the amplitudes of the reflections from below the EB are not unusually small, but rather the EB reflects unusually strongly. Structures in the lower crust cannot be resolved by the selected offsets (in contrast, see Fig. 42c). A linear relationship from 5.8 km/s at $T_{mod} = 2$ s to 6.25 km/s at $T_{mod} = 12$ s is assumed for the correction velocity V_{mod}; **b** The vicinity of the EB imaged by three different wide-angle COF sections; in this case a constant value of 5.95 km/s was applied as the correction velocity. The influence of the offsets and the different angle of incidence, respectively, cause different results; **c** Dynamically corrected COF sections, obtained from MARS observations at distance intervals (72±1) km, *top*, and (82±1) km, *bottom*. Through these offsets, the lower crust (at about 7 s) and the Moho (at 10–11 s) can be imaged, whereas the upper crust can no longer be resolved. Below the EB, the lower crust appears at a depth of about 23 km

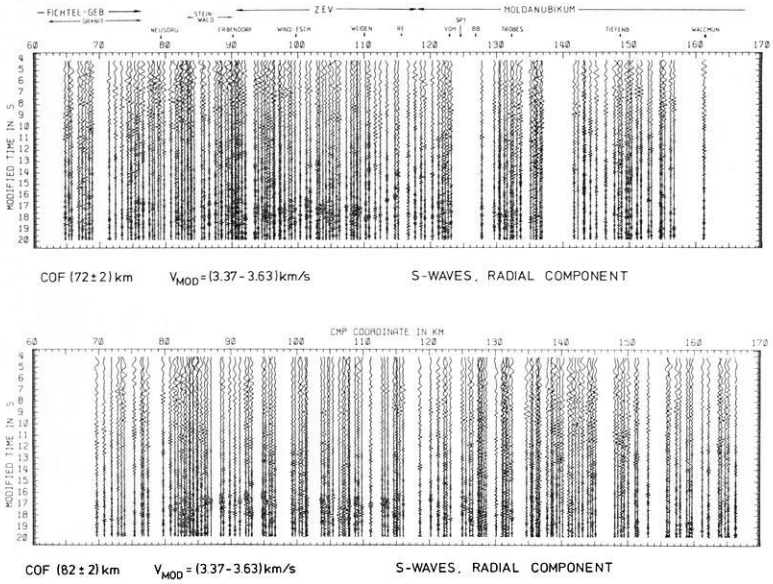

Fig. 43. Dynamically corrected *S*-wave COF sections for offset ranges 72 ± 2 and 82 ± 2 km. The time scale and the correction velocity V_{mod} have been chosen so that the same image should result as in Fig. 42c if the V_p/V_s relation in the whole crust were 1.72. However, the lower crust is, surprisingly, not imaged by the *S* waves, whereas the Moho in the ST/MN boundary domain becomes more clearly recognizable as an updoming than through the *P* waves

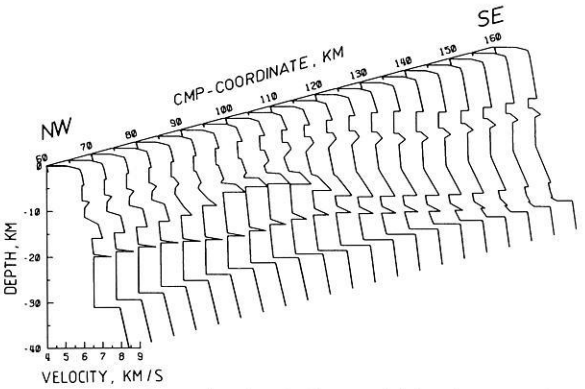

Fig. 44. Two-dimensional velocity model for the DEKORP 4 profile between profile km 60 (Gefrees) and 160 (Waldmünchen). Velocity-depth functions at intervals of 5 km

along the DEKORP 4 line on the basis of the previously explained qualitative findings and a large number of velocity analyses from CMP wide-angle sections and reversed observations, as well as results of earlier work (Stroessenreuther, 1982). The model was improved iteratively by extensive ray-tracing computations; the interpretation has not yet been completed. Nevertheless, the travel times of the most important wave groups in the essential parts of the profile have already been satisfactorily explained, i.e. within ± 0.1–0.2 s. Thus, the velocity model of Fig. 44 can, in essence, be regarded as well founded. The velocity modelling to obtain this two-dimensional velocity distribution has been performed with a new technique (Gebrande and Bopp, in preparation).

Superposing the velocity-depth functions, converted to two-way travel times, over the line-drawing of the near-vertical seismics is very informative; the result (Fig. 45) shows a remarkable coherence between the structural elements and the seismic velocities.

In view of the decision to sink the KTB borehole in the immediate vicinity of Erbendorf, particular importance is attached to the EB. To explain the high apparent velocities of the wide-angle reflections that were observed in CMP and CSP sections, as well as in sections with common receiver points, the EB was modelled as a high-velocity body with *P*-wave velocities between 7.0 and 7.5 km/s, with its top at a depth of about 12 km (Fig. 44). Through the computation of synthetic seismograms, Sandmeier and Wenzel (personal communication) have shown that the chosen velocity distribution also explains the high amplitudes of the wide-angle reflections observed. However, this does not mean that a proof has been furnished therewith for the existence of a high-velocity body. Sandmeier and Wenzel (personal communication) have also shown that, theoretically, a stack of dipping lamellae with alternating velocities of 5 and 6 km/s can also produce the observed high apparent velocities and amplitudes. In fact, a lamination, as otherwise typical for the lower crust, is quite probable from the near-vertical reflection seismic image of the EB, especially on profile KTB 8505 (Fig. 25). However, the dips necessary for such lamellae models cannot be confirmed by the wide-angle image.

In detail, the velocity analyses of wide-angle seismics for the area around Erbendorf (CMP 90) show stronger heterogeneity (Fig. 46) than the relatively smooth velocity model of Fig. 44. Different results for slightly deviating travel-time correlations and various methods of inversion (Fig. 46) show that such details cannot be reliably resolved from wide-angle travel times. Nevertheless, it is worth noting that interval velocities above 7 km/s at depths of 12.5–13.5 km (the thick curve in Fig. 46) also result from investigations by Gebrande and Bopp (in preparation). The existence of high rock velocities, which are observed elsewhere in the lower crust only, thus becomes highly probable for the basal part of the EB. Whether tectonically displaced lower-crustal material is actually involved can certainly not be decided solely through observations at the surface.

The velocity model presented in Figs. 44 and 46 contains the entire inventory of crustal seismic structural elements in the upper 15 km: high- and low-velocity zones, discontinuities and gradient zones; that lamellae zones exist is highly probable. The significance of the observation data leads one to expect that the essential structural elements are particularly clearly developed in the location area. These are favourable prerequisites for obtaining extensive new knowledge about the true nature of seismic inhomogeneities and reflectors in the crystalline basement through the KTB.

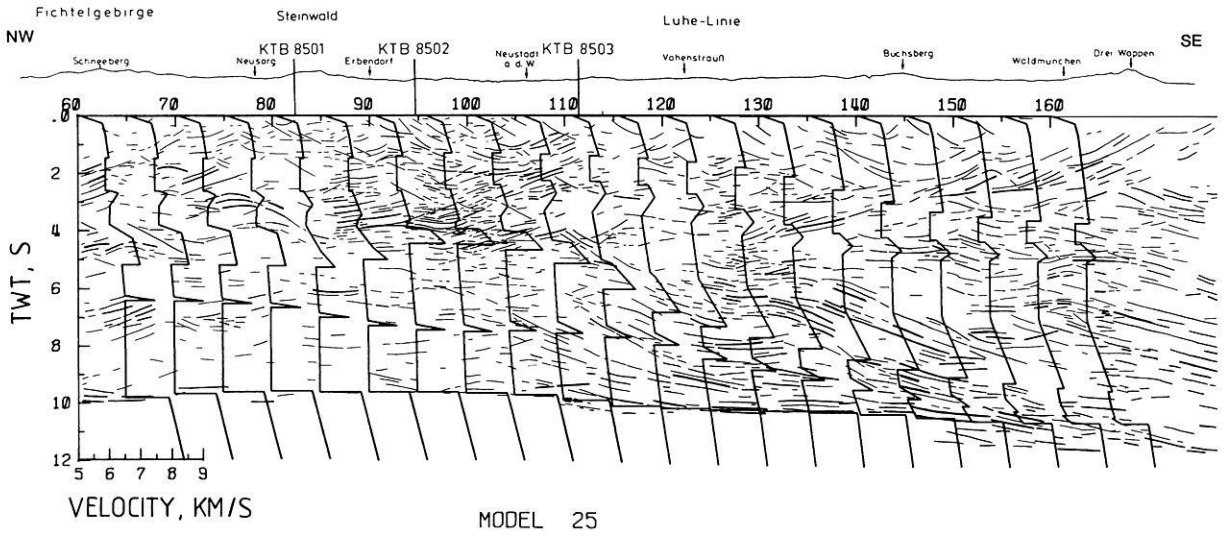

Fig. 45. Superposition of the velocity-depth functions of Fig. 44, converted to two-way travel time on the line-drawing of near-vertical seismics from Fig. 6

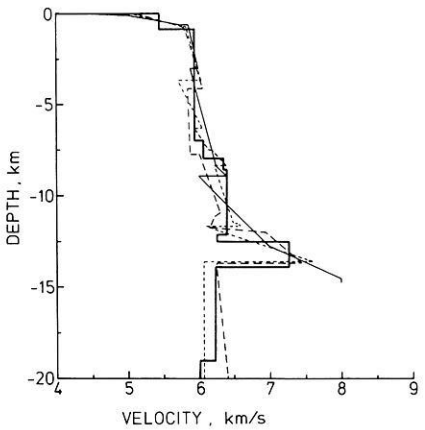

Fig. 46. Velocity-depth functions that were obtained for CMP 90 according to different interpretation techniques and for slightly differing travel-time correlations. The bandwidth of the solutions gives an idea of the resolving power of wide-angle seismics in the upper crust. All solutions have velocities larger than 7 km/s in the lower part of the EB at depths of 12–13 km

4.3 Results of the expanding spread experiment

The data of these experiments (see Section 4.1; Fig. 36) were sampled at 4 ms over the record length of 40 s. A bandpass filter of 5–32 Hz was used, the dominant signal frequency being around 20 Hz. For the interpretation of *P* waves, the record length was reduced to 20 s. Problems for data processing and interpretation were low signal/noise ratios, insufficient statics information, varying frequencies and wave forms (due to different equipment and coupling effects) and the very heterogeneous crust in the vicinity of the boundary between MN and ST. Thus, the chance of destroying signals by stacking of adjacent traces was quite high. Therefore, a special technique was applied using the "energy" characteristics of traces: squared amplitudes were normalized with regard to the maximum energy per trace. Subsequent mixing and smoothing by use of two moving windows over five traces and 80 ms resulted in the energy sections shown in Fig. 47. First arrivals can be observed very clearly up to a distance of about 60 km in the southern part (MN). After some near-vertical reflection bands (P_c) from the lower crust in the offset range 20–55 km, the Moho reflection (P_mP) appears really strong in the near-vertical and wide-angle range.

In the northern part (ST) clear first arrivals can be observed up to a distance of 65 km. Here, only one strong reflection band (P_c) appears in the lower crust. In addition, there are weak indications for upper-crustal reflections and the P_mP.

Using squared amplitudes and moving windows, the picking of exact arrival times becomes difficult. Therefore, an "energy controlled gain" (ECG) was applied to the original traces (Bittner, in preparation). Due to this procedure, phases and arrival times are not distorted. Figure 48 shows the effect of this processing to selected parts of the seismogram sections from the ST domain (top) and the MN domain (bottom). A clear improvement is obvious: now several reflections can be followed after the first arrivals.

Figure 49 gives the results of a 1-dimensional interpretation consisting of a direct inversion of first arrivals combined with RMS velocities derived from x^2/t^2 values using the reflections of the entire sections shown in Fig. 47. In order to gain 2-dimensional velocity information, common-shot gathers (CSG) were constructed from single shots along the profile and 2-dimensional ray tracing was used. This investigation is not finished, yet, but first estimations were included in the 1-dimensional velocity-depth structure. Figure 50 shows the interval velocities derived from 1-D and 2-D inversions for the two ESPs.

For both ESPs a low-velocity zone appears in the depth range 5–10 km, but which is more pronounced in the MN. Comparing these two velocity-depth functions, there are no "typical" structures for the Moldanubian and Saxothuringian. A separation into upper and lower crust is not obvious. The mean velocities of the whole crust are identical: 6.25 km/s. The two ESP velocity-depth functions are similar, but not identical, to the 2-dimensional model of Fig. 44 at the appropriate locations. The high-velocity body has about the same depth and thickness in both interpretations; it is to be correlated with the observations of the EB at the KTB drilling site between the two ESPs.

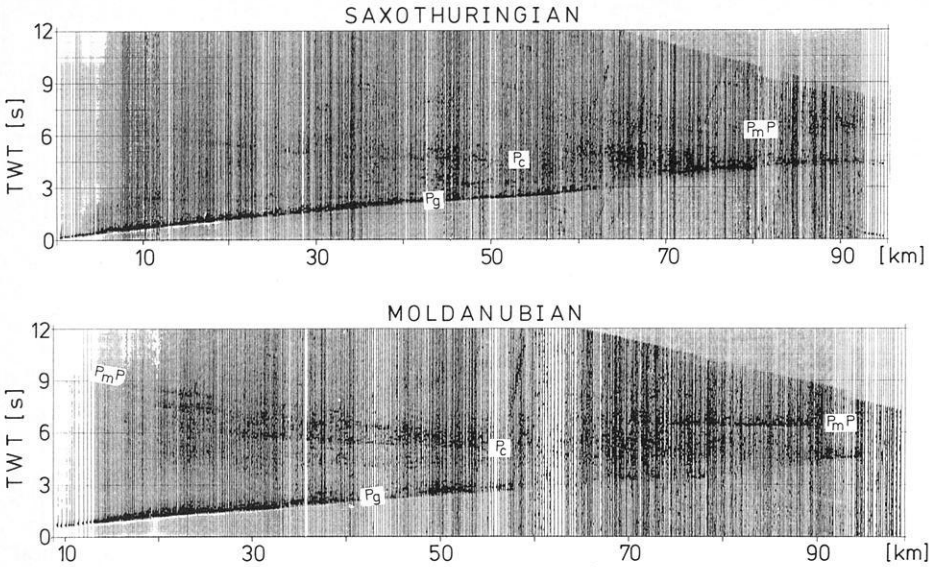

Fig. 47. Energy sections for the Saxothuringian (*top*) and the Moldanubian (*bottom*); time coordinate reduced by 8 km/s. For these sections, squared amplitudes and a moving window over five traces and 80 ms was used

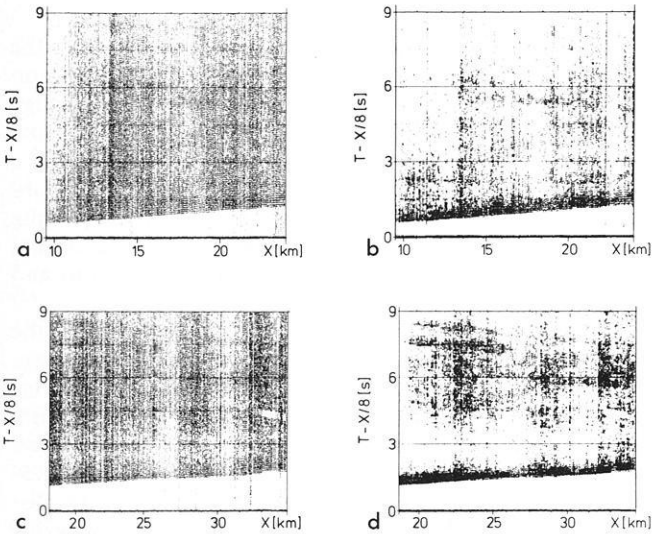

Fig. 48a–d. Original traces (**a, c**) for the ESP of the Saxothuringian (*top*) and the Moldanubian (*bottom*). Corresponding "ECG" traces (**b, d**) of the two corresponding ESPs. An energy controlled gain was applied by multiplication of the original traces (**a, c**) with the energy traces. Phases and arrival times are not distorted

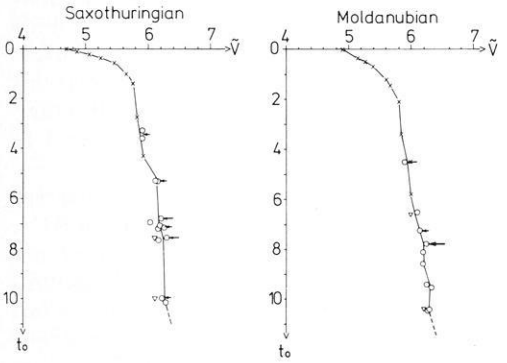

Fig. 49. RMS velocities derived from x^2/t^2 values using the reflections observed on the energy and ECG sections. *Crosses:* direct inversion of first arrivals (1-D); *circles*: RMS velocities from x^2/t^2 values; *triangles:* optimum stacking velocities from stack tests; *arrows:* dip corrections, computed from the migrated section of DEKORP 4 (RMS velocities divided by the cosine of the dip angle)

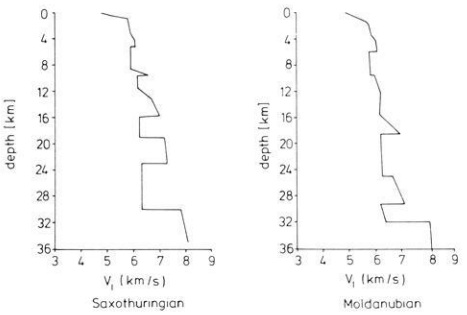

Fig. 50. Computed interval velocities for the two CMPs (*left:* Saxothuringian; *right*: Moldanubian). 1- and 2-dimensional inversion methods were used

5 Attempt at tectonic interpretation

5.1 General introduction; the northern part of DEKORP 4

SE-dipping reflectors are present in all NW/SE reflection seismic profiles (DEKORP 4, KTB 8504–8506). These reflectors confirm the extensive overthrusting of Moldanubian crust onto Saxothuringian crust interpreted from the geology at the surface: the ST/MN boundary is a tectonic suture zone (Fig. 51).

There are also NW-dipping reflectors, particularly on the DEKORP 4 profile. These reflectors, together with subhorizontal reflectors occurring in various sections of the seismic profile, can be interpreted in several ways.

At first glance, the following structural units can be recognized on the DEKORP 4 profile (see Fig. 51). The MM and ZEV nappes clearly form bowl-shaped structures. The base of the synformal MM is more distinct than that of the ZEV. This can be explained by the fact that the gneisses of the MM are underlain by anchimetamorphic sediments; whereas the ZEV rocks, at least in their southern part, rest upon Moldanubian gneisses of similarly high metamorphic grade. In the anchimetamorphic sediments of the Frankenwald northwest of the MM there is a reflection horizon at about 1 s TWT which passes southeastward under the MM and can be correlated with the boundary between Upper-Devonian (Frasnian) spilites and the overlying late-Devonian and Lower-Carboniferous sediments.

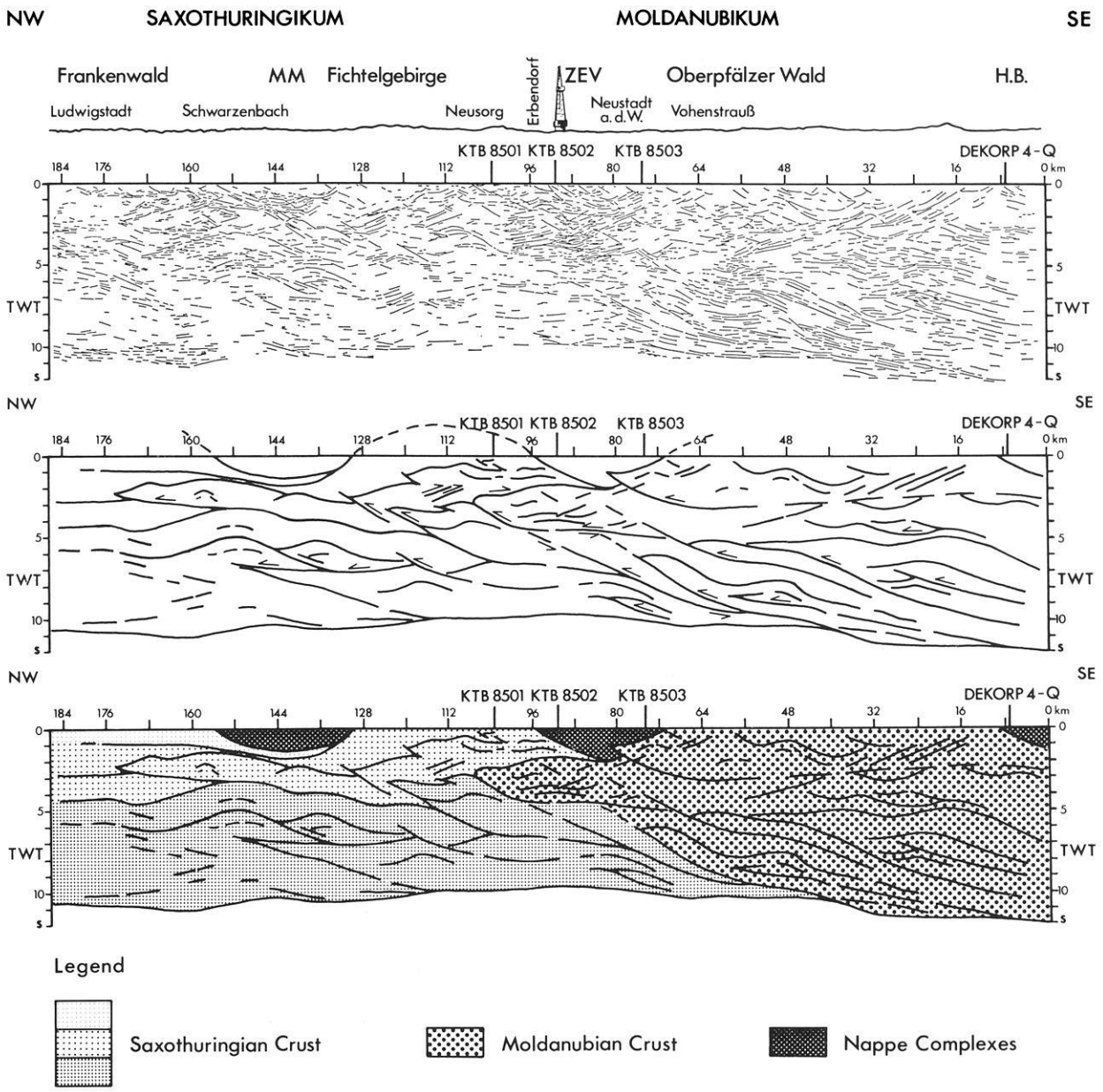

Fig. 51. Line-drawing of profile DEKORP 4, derived from the migrated and coherency-filtered section (*top*). *Centre and bottom:* preliminary structural model based on the line-drawing. *MM* – Münchberg Massif; *ZEV* – Zone of Erbendorf-Vohenstrauß; *HB* – Hoher Bogen

The ST region at middle- and upper-crustal levels is characterized by extensive, slightly asymmetric pre-deformed structures with a dominance of SE-dipping reflectors. Under the MN region this dominance of SE-dipping reflectors increases very clearly. On the other hand, in the upper-crustal levels a structural discontinuity can be recognized, starting at the base of the EB and continuing to the southeastern end of the section. Above this discontinuity NW-dipping reflectors and extensive previously deformed structures dominate, especially in the south.

There are several possibilities for interpreting these structures. In the line-drawings in Fig. 51 not only can the MM, ZEV and HB nappes be recognized, but MN and ST crust can be differentiated as well.

A subdivision of the ST crust into three different layers is attempted. The uppermost layer at the northwestern end of the section represents the anchimetamorphic sediments of the Frankenwald above the prominent reflector at about 1 s TWT, i.e. above the presumed Frasnian spilites. The second layer is formed by the supposed equivalents to the Early-Palaeozoic to Upper-Proterozoic (?) metasediments of the Fichtelgebirge below the spilites. At the NW end of the profile, the third relatively homogeneous crustal level with predominantly SE-dipping reflectors is indicated below 4 s TWT. Possibly a pre-Variscan basement is reached here, whose Variscan overprinting by NW-vergent folding and thrusting increases clearly to the SE.

The anticlinal structure under the northwestern part of the Münchberg nappe complex (at about km 150) is presumably a more or less autochthonous structure. This is supported by a correlation with the SW-plunging Hirschberg-Gefell Anticline at the surface. Support is also offered

by the fact that this anticlinal structure, whose NE-striking extension can be traced to the Saxonian Granulite Mountains, is the source area for the Upper-Devonian conglomerates of the Frankenwald (Franke, 1984a). This interpretation is also advocated by the northwestward and southeastward increase in thickness of the metasediments away from the core of the anticlinal structure.

The SE-vergent D_2 folding of the Frankenwald and the Fichtelgebirge is not expressed in the seismic structure of any of the NW/SE profiles. Only in the ST portion of the DEKORP 4 profile down to about 3 s TWT can NW-dipping reflectors, which may be interpreted as SE-vergent structural elements, be recognized.

In the NW section of the DEKORP 4 profile around km 168 these SE-vergent structures can be assigned to the NW flank of the large anticlinal structure under the northwestern MM. Thereby the SE-vergent D_2 folds of the Frankenwald can be interpreted as adventive folds on the NW flank of a very large anticlinal structure, which would then be a D_2 structure. That this structure is, as a whole, NW vergent, is shown by the configuration of the reflectors in the northwesternmost upper part of the structure which can be interpreted as a subhorizontal NW-vergent overthrust (Fig. 51, bottom). This overthrust has displaced the upper part (widely dotted) of the anticlinal core to the northwest relative to the lower part (closely dotted). The asymmetry of the possible duplex structure below 5 s TWT indicates the same direction.

The Vogtland syncline, in which the MM is preserved, is a post-nappe (possibly D_2) structure, whereas the Fichtelgebirge anticline clearly represents a D_3 structure (Stein, 1987). The core of the Fichtelgebirge anticline with the stratigraphically oldest, exposed rocks (Stettner, 1972) coincides with the core of this structure on the DEKORP 4 profile (Fig. 51) at about 110 km. The main elevation of the Fichtelgebirge composed of granites is situated on the NW flank of the Fichtelgebirge anticline. The great extent of granites is indicated, on the DEKORP 4 profile, by a relatively transparent domain between 112 and 128 km and down to 2 s TWT.

5.2 The structure of the Erbendorf area

From the central Fichtelgebirge to the SE, the SE-vergent D_2 deformation gains importance. A possible explanation for this SE-vergent D_2 structure, which is time-equivalent with the peak of metamorphism in the southern Fichtelgebirge, is given by the interpretation of the EB.

If the EB is interpreted as part of the MN crust based on its seismic structures, it extends into the ST zone and must be underlain and overlain by ST rocks (Fig. 51). Thereby the picture of a MN crustal wedge which has penetrated ST crust has developed. This type of wedge tectonics, or flake tectonics in the sense of Oxburgh (1972), is also known from other orogenic belts (Price, 1986; Brown et al., 1986) and explains both the seismic crustal structure and the pronounced SE vergence of the D_2 deformation in the central and southern Fichtelgebirge, as well as the lack of this pronounced SE vergence on the NW flank of the Fichtelgebirge. The MN crustal wedge presumably penetrated into the middle ST crust along a structural or lithological discontinuity between a metasedimentary cover and a pre-Hercynian basement during D_2 deformation.

The relative southeastward movement at the top of this wedge led to the SE-vergent D_2 folding in the Fichtelgebirge. This movement picture is similar to that of a passive-roof duplex, as described by Banks and Warburton (1986) for Pakistan. At the bottom of the wedge, northwestward overthrusting and southeastward underplating continued during the wedging.

Due to its velocity structure, the basal part of the EB could be composed of lower-crustal material, e.g. of mafic to ultramafic magmatites, or garnet-sillimanite-rich metapelites which can have compressional velocities of over 7 km/s according to Kern and Schenk (1985).

The internal structure of the EB shows SE- and NW-dipping reflections in addition to the predominantly horizontal ones (Fig. 11). A distinct NW boundary cannot be recognized. In Fig. 51 the NW end lies in a relatively transparent zone which conforms to a SE-dipping, ramp-shaped seismic structure. The seismic transparency is possibly the result of a particularly intense internal deformation of this frontal portion of the EB.

Individual tectonic structures can be reconstructed at upper- and middle-crustal levels of the ST part of the profile, using the position and orientation of the reflectors. In the lower crust, however, a relatively homogeneous, SE-dipping structural pattern dominates. Correlation with structures at the surface is not possible. The slightly SE-dipping reflectors which then become horizontal near the Moho are indicative of a flow regime which sustained constant, relative movements between the crust and mantle. This is also true for the lowest MN crust.

The boundary between the ST and MN below the EB is not yet clearly recognizable despite the general differences in their seismic structures. This boundary presumably lies where the relatively transparent crustal zone with mainly low-angle SE-dipping reflectors borders the strongly reflecting crustal zones marked by imbricate fold and ramp structures. The style of deformation of the lower MN crust presumably passed over into the lower ST during the collision process. At the boundary zone, where MN overrode ST rocks, strong imbrication may be assumed.

In the MN there is a structural discontinuity at about 4–5 s TWT, below which SE-dipping reflectors predominate. In the hanging wall, strong NW-dipping reflectors, such as those observed near the EB below the ZEV, occur in addition to subhorizontal, slightly sinuous reflectors (e.g. between km 32 and 56).

These NW-dipping reflectors could be SE-vergent overthrusts genetically related to the SE-vergent D_2 structure of the Fichtelgebirge. Although the SE-vergent D_2 structures at the surface of the Fichtelgebirge are the dominant features, they are hardly expressed in the seismic pictures of DEKORP 4 and KTB 8504–8506. It would be all the more surprising if there were SE-vergent overthrusts in the MN which could neither be observed in the field nor deduced from a geological map in the area of DEKORP 4.

However, SE-vergent structures are widely distributed in the MN and ST of the Variscan orogeny. Thus, it can be imagined, alternatively, that the clearly N-dipping reflectors, which rise from the EB southward to the southern margin of the ZEV, represent S-vergent overthrusts. Southward-directed folding and thrusting has also been proposed for the southern margin of the Tepla-Barrandean in Czechoslovakia (Tollmann, 1982), which can be regarded as an eastward equivalent of the ZEV.

It has been confirmed in the ST and northern MN that the SE vergence belongs to the deformational phase D_2. In the central and northern ST, the age of the collective D_1 and D_2 deformation is stratigraphically limited to the uppermost Lower Carboniferous (about 320–330 Ma; Franke, 1984a). In the Fichtelgebirge, the syn-D_2 metamorphism has been dated at ± 320 Ma (Teufel, 1987). The shearing which occurred during the emplacement of the Bohemian granulite nappe was dated at ± 341 Ma by van Breemen et al. (1982).

All S-vergent elements appear to be of the same age (within geochronological error bounds) and it is therefore possible that they belong to the same event which is younger than the D_1 deformation in the ST. Since D_1 is doubtlessly N vergent, this would imply a reversal of the direction of overthrusting, as known from other orogenies. During the subsequent deformation, a NW-vergent sense of shear has been resumed (D_3), although with much shorter transport distances. During the indentation stage of collision (D_4), a SW-vergent sense of overthrusting developed (Weber, 1986).

For the geotectonic interpretation of the EB, this would mean that its roof and base were not active at the same time, but that the roof experienced younger backthrusting. This would not be wedge tectonics in the true sense, but would mean that the wedge form was a product of two successive acts of deformations.

From this point of view, the metabasite of the Erbendorf greenschist zone could be interpreted to represent the original, near-surface extension of the EB. The mafic and ultramafic rocks near Erbendorf and their equivalents in the Münchberg units (serpentinites, amphibolites) fit well into this hypothesis. In this sense, the Erbendorf line would be the root zone of the MM displaced southeastward through backthrusting.

However, at least a part of the N-dipping reflectors can be interpreted with concepts other than backthrusting. Comparison with the ZEV (Fig. 52) shows the trend of the metamorphic s-planes in the Moldanubian part of DEKORP 4. The ZEV is bowl-shaped in the seismic profile. In contrast to the MM, the ZEV is not a NE- to SW-striking but a generally NW- to SE-striking D_4 syncline. Correspondingly, in the DEKORP 4 profile the synclinal shape results from SE-dipping reflectors in the northwest, horizontal reflectors in the middle and NW-dipping reflectors in the southeast.

In the area of the Naabgebirge block (NGS in Fig. 52), there is an analogous situation between the Luhe Line and Hoher Bogen. Here, the NW- to SE-striking, SW-vergent structure (D_4 in the MN of the Oberpfalz) gains increasingly in intensity southeastward toward the Bavarian zone. The DEKORP 4-Q profile (Fig. 17) shows that the SW-vergent structure of the Bavarian zone can be correlated with NE-dipping listric reflectors which join at about 3 s TWT into a bundle of prominent, horizontal reflectors. Around the Naabgebirge the arc-shaped strike of the s-planes, which generally dip northeastward, indicates an anticlinal structure in the north, a synclinal structure in the central portion and an anticlinal structure in the south just before Hoher Bogen, a part of the ZTT nappe. This can be regarded as the result of a large-scale undulation of the axis of the generally NW- to SE-striking large-scale fold structure. The large-scale folds seen in the DEKORP 4 profile are clearly recognizable between km 32 and 56.

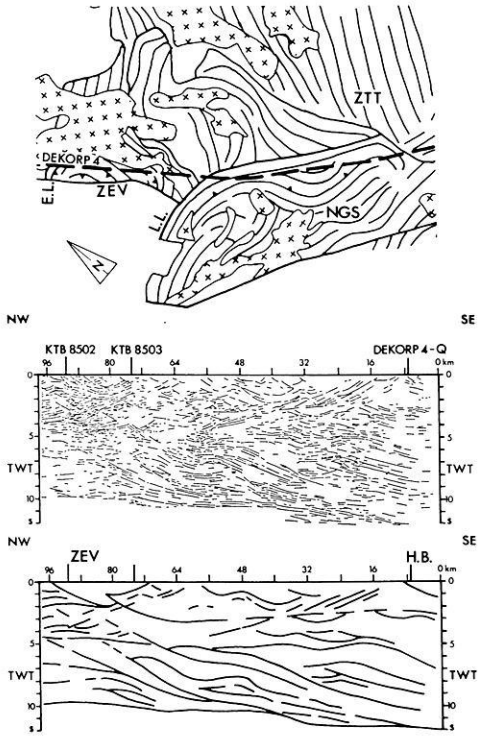

Fig. 52. Correlation between changes in dip and strike of tectonometamorphic s-planes in the MN part of DEKORP 4 (*top*) and dipping reflectors above 4–5 s TWT (*centre:* line-drawing). Additionally, the structural model of the corresponding part of DEKORP 4 is shown in the *lowest part* of the figure

The ascent of the reflectors toward the southeast and northwest thus results from the DEKORP 4 profile running obliquely through the SW-vergent (NE-dipping) structures.

SW-vergent overthrusts, like those in profiles KTB 8501–8503 and DEKORP 4-Q (see Section 3), presumably belong to these reflectors as well. A sinistral deviation in their strike from the path of DEKORP 4 always leads to lines ascending southeastward, whereby the acute angle between the strike and DEKORP 4 causes the more frequent occurrence of side reflections.

The above interpretation is supported by the observation that NE-dipping reflectors and SW-vergent overthrusts in KTB 8501–8503 only occur more frequently above about 4–5 s TWT and join horizontal reflectors at 3–5 s TWT. This level corresponds approximately to the base of the EB between km 80 and 96 and a structural discontinuity with SE-dipping reflectors in the lower part and horizontal to NW-dipping reflectors in the upper part between km 56 and 80.

Southeast of km 56, there is a bundle of NW-dipping reflectors which are interpreted as NE-dipping structures cut at an oblique angle, as in the interpretation above. In the DEKORP 4-Q profile, which is perpendicular to the NW/SE strike of the "Pfahl" mylonites, the NE-dipping reflectors at about 2.5–3.0 s TWT pass into a prominent horizontal bundle of reflectors, which corresponds to the structural discontinuity at the SE end of DEKORP 4 at this depth (Fig. 51).

In the ST north of the Fichtelgebirge, the nappe transport has been dated as late Lower Carboniferous (320–330 Ma, Franke, 1984a). It is older than the oldest posttectonic granites which are dated at 320 Ma.

The lithologies, metamorphic development and radiometric ages have proved that the MM and ZEV had the same evolution and origin. Behr et al. (1982) and Franke (1984a) regard the Erbendorf line at the NW margin of the ZEV as the tectonic suture marking the root zone of the MM. The existence of a nappe complex (ZEV) originating from and south of this root zone might be explained by D_2 backthrusting. Nappe transport must have occurred before the low-pressure (LP) metamorphism of the Fichtelgebirge and of the MN of the Oberpfalz since the nappes were not affected by this metamorphism. The base of the ZEV may have undergone a LP metamorphic overprinting, as indicated by the younger hornblende ages at the southern margin of the ZEV. However, a possible cause for these younger ages may also have been contact metamorphism produced by the adjacent Oberpfalz granite (Schüssler et al., 1986).

Zoubek (1979), Stettner (1979) and Blümel (1985) have pointed out the lithofacies and metamorphic relationship of the medium-pressure (MP) metamorphic ZEV and MM to the likewise MP metamorphic ZTT (Fig. 52) and inferred a formerly coherent MP metamorphic nappe complex which overlies the MN of the Oberpfalz and the Fichtelgebirge. Yet, the position of its root zone is, at present, uncertain.

The results of DEKORP 4 and the KTB seismic profiles may be taken to indicate that the ZEV overlies the ST/MN boundary in the form of a NW- to SE-striking syncline. In this sense, the "Erbendorf Line" would correspond to the boundary between the ZEV nappe and the ST rocks of the Fichtelgebirge, and not to a tectonic suture as previously assumed.

Orogenic shortening began with NW-vergent folding and thrusting. During continued collision, the style of deformation along the ST/MN boundary zone is increasingly controlled by crustal wedging, resulting in backfolding above the EB and continuous underplating or subfluence of ST under MN crust. This homo-axial structuring of the first and second phase of deformation is continued by the large upright, NE- to SW-striking folds of the third phase of deformation. During the fourth phase of deformation in the ST and MN zones, N/S- to NW/SE-striking, low-sinuous folding took place, which decreases in intensity to the NW.

5.3 Discussion on effects of possible indentation processes

NW- to SE-striking structures occur more often south of the Luhe line. In the southwestern, marginal part of the Bohemian Massif (Bavaricum), NW- to SE-striking structures in the form of pronounced mylonitization near the Bavarian "Pfahl" dominate. These NW- to SE-striking structures are SW vergent and have overprinted older NE- to SW-striking structures. In profile DEKORP 4-Q (Fig. 17) these SW-vergent structures are very clearly depicted by NE-dipping reflectors. One NE-dipping reflector can be correlated with the "Pfahl" mylonites at the surface and can be connected to the northeast to a listric overthrust with a subhorizontal reflection horizon at about 3 s TWT.

In sections KTB 8501–8503, E-dipping reflectors are recognized, particularly east of the Franconian line (Figs. 18–22). Prominent reflectors below 2 s occur, especially in section KTB 8502. These reflectors are intersected by steep,

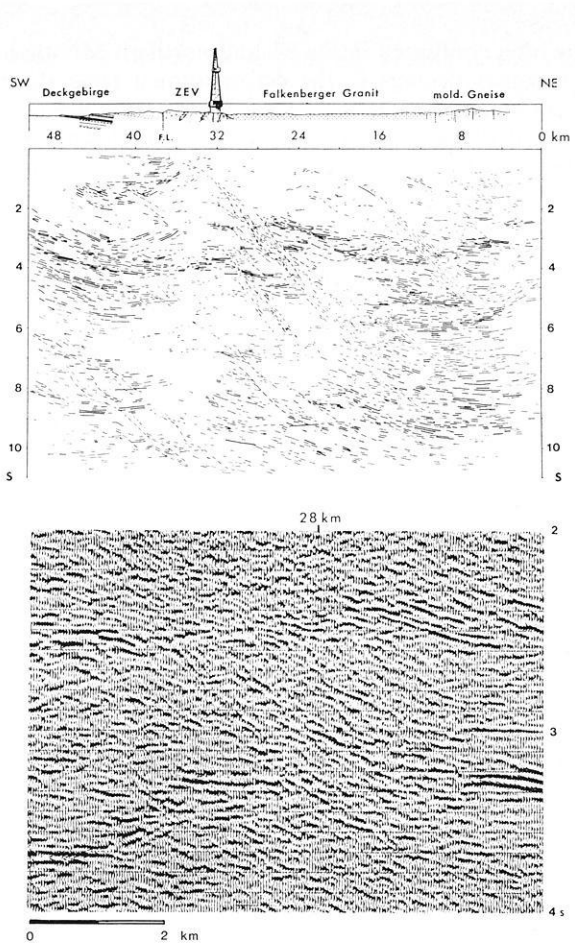

Fig. 53. Line-drawing of profile KTB 8502 (migrated section) and (*bottom*) detail of the section between 2 and 4 s below km 28 showing NE-dipping reflections which cut through strong, more or less horizontal reflectors. The internal structure of this fault zone is similar to that of the Pfahl mylonites in DEKORP 4-Q. It is interpreted as a ductile shear zone

E-dipping, relatively transparent zones which are composed of numerous E-dipping reflectors.

These transparent zones give the impression of zones of faulting in which the prominent subhorizontal reflectors are obliterated (Fig. 53). These relatively young, NW/SE- to N/S-striking structures are assumed to be equivalent to the NW- to SE-striking structures appearing at the surface. Thus, they could be assigned to the D_4 structures of the ST and MN boundary zone of the Oberpfalz (Stein, 1987) as well as the dominant NW/SE structures south of the Luhe line (DEKORP 4-Q). They are presumably zones of ductile shear, like those observed in the mylonite zone along the Bavarian "Pfahl".

Whereas SW vergence is observed on the SW margin of the Bohemian massif, SE-directed tectonic transport occurs in the region of the southern Black Forest, particularly in the area of the Zinken-Elme and the Badenweiler-Lenzkirch shear zone (Eisbacher and Krohe, 1986). The gravimetric and magnetic anomalies of the pre-Mesozoic basement between the Black Forest and the SW margin of the Bohemian massif reveal contours to the north, outlining the structural grain of the pre-Mesozoic basement (Edel, 1982). This arc structure is also seen in the form of the Permo-Carboniferous troughs in the region of the Southern German Massif (Fig. 54).

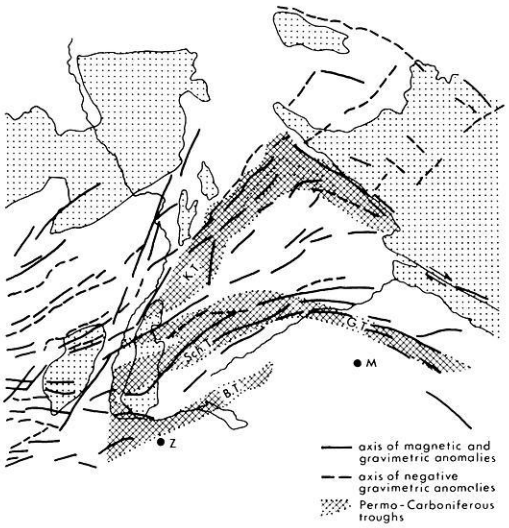

Fig. 54. Axes of magnetic and gravimetric anomalies and corresponding arc structure of Permo-Carboniferous troughs between Bohemian Massif and Black Forest. *B.T.* – Bodensee Trough; *Sch.T.* – Schramberg Trough; *G.T.* – Gifttal Trough; *K.T.* – Kraichgau Trough

As in the case of the Himalayas or the Ibero-Armorican arc (Taponnier and Molnar, 1976; Matte, 1986a), this structure can be interpreted after Weber (1986) as an indentation structure. Collectively, the arc shape of the suture zones around the various terranes of the European Variscan Belt is controlled by this later indentation process, presumably extending into the Upper Carboniferous. The indentation structures generally developed from a rather cylindrical configuration of the entire orogeny. This can explain the overprinting of older NE- to SW-trending structures by younger NW/SE structures along the southwestern margin of the Bohemian Massif by which the tectonic transport changes from SE/NW to NE/SW on the SW margin of the Bohemian Massif, and from SE/NW to NW/SE in the Black Forest. The NW-dipping reflectors in the Oberpfalz represent these thrusts formed during the indentation stage of the Vindelician Massif, which may be traced into the Hercynian basement of the Eastern Alps.

Further manifestations of the indentation process are the large dextral and sinistral shear zones. The dominance of dextral shear zones in the eastern part of central Europe, as also shown by Arthaud and Matte (1977), resulted from the movements of the terranes relative to the East-European platform. In detail, the dextral movements on the Bavarian mylonites and the sinistral movements between the Black Forest and Vosges can be assigned to the indentation process of the Vindelician Massif. During the indentation process, sutures can be transformed into wrench faults and orthogonal collision can be transformed into oblique collision.

A further argument for such an indentation structure is the rotation of the magnetic declination which is observed on both sides, but in opposite directions. In the southern Vosges Edel et al. (1984) have shown that the mean direction ($D = 323°$) deviates about 60° counterclockwise from the theoretical direction calculated with the Early-Carboniferous European pole position. This deviation is interpreted as resulting from a counterclockwise rotation of the southern Vosges between the late Visean and Westphalian. The same sense of rotation was also determined by Royer (1982) in the northern Vosges and by Bosum et al. (1973) in the crystalline Spessart.

In contrast, the rotations of the magnetic declination in the region of the Bohemian Massif amounted to 20°–35° in a clockwise rotation during the Carboniferous and the Permian as shown by the studies of Krs (1978) and Kim and Soffel (1982). The sense of shear and rotation of magnetic declination does agree very well with the presumed indentation process. The rotation of magnetic declination is very analogous to that in northern Spain where it indicates the virgation of the Iberian arc (Ries et al., 1980; Perroud, 1982).

5.4 Conclusions

From the interpretation given here it can be seen that there are still many open questions regarding the geotectonic evolution of this region. Nevertheless, there is currently a good consensus on the basic elements of the crustal structure which is summarized in the following.

The crust is marked by northwestward overthrusting, whereby Moldanubian crust has overridden Saxothuringian crust. Tectonic deformation and the accompanying metamorphism are multi-phase. During the D_2 deformation there were also southward movements, at least in places. This has affected the northward penetration of a wedge of probably Moldanubian crust with partly higher seismic velocities into the Saxothuringian in the region of the EB.

The dominant, open, large-scale folds seen on the geological map and in the seismic profiles are the product of younger deformations (D_3, D_4) whereby, at lower-crustal levels, folding has been compensated to some extent by overthrusting, also seen in the seismic sections. The large-scale nappes are older than the D_4 deformation. This interpretation seems to be well justified by the excellent correlation between the surface geology and seismic data.

Acknowledgements. The continued funding of the DEKORP project by the Bundesministerium für Forschung und Technologie, Bonn, is gratefully acknowledged. Administrative services were provided by the Niedersächsisches Landesamt für Bodenforschung, Hannover. The excellent performance of the Prakla-Seismos AG field crew under H. Schwanitz was remarkable, and there was smooth cooperation between the various groups in the field. The Raytheon RDS 500 is a donation of Mobil Oil AG Celle to the DEKORP Processing Center at Clausthal. The software was provided by Seismograph Service Ltd., London. BEB Erdgas und Erdöl GmbH, Hannover, supported the work by special processing. The close cooperation with Preussag AG was very helpful. Special thanks are due to the large number of students participating in the field work and all members of the DPC.

References

Ackermann, H., Tavakkoli, P.: Granite – Form und räumliche Lage im metamorphen Grundgebirge. Abstracts, 76. Jahrestg. Geol. Vereinig., Giessen 1986, 1, 1986

Arthaud, F., Matte, Ph.: Late Paleozoic strike slip faulting in Southern Europe and Northern Africa: result of a right lateral shear zone between the Appalachians and the Urals. Geol. Soc. Amer. Bull. **88**, 1305–1320, 1977

Banks, C.J., Warburton, J.: "Passive-roof" duplex geometry in the frontal structures of the Kirthar and Sulaiman mountain belts, Pakistan. J. Struct. Geol. **8**, 229–237, 1986

Behr, H.J., Engel, W., Franke, W.: Variscan Wildflysch and nappe

tectonics in the Saxothuringian zone (Northeast Bavaria, West Germany). Amer. J. Sci. **282**, 1438–1470, 1982

Behr, H.-J., Engel, W., Franke, W., Giese, P., Weber, K.: The Variscan Belt in Central Europe: main structures, geodynamic implications, open questions. Tectonophysics **109**, 15–40, 1984

Besang, C., Harre, W., Kreuzer, H., Lenz, H., Müller, P., Wendt, I.: Radiometrische Datierung, geochemische und petrographische Untersuchungen der Fichtelgebirgsgranite. Geol. Jb. **E 8**, 3–71, 1976

Blümel, P.: Metamorphic history. In: Excursion guide Oberpfalz, Weber, K.: 2nd Inter. Symposium on observation of the continental crust through drilling. Seeheim/Odenwald, 7–9 October, 1985, 23–30, 1985

Bopp, M.: Analyse und Interpretation von S-Wellenregistrierungen im Rahmen des Deutschen Reflexionsseismischen Programms DEKORP. Dipl.-Arbeit, Ludwig-Maximilians Universität, München, 1986

Bosum, W., Geipel, H., Weinelt, W.: Magnetische Untersuchungen im kristallinen Spessart und ihre geophysikalisch-geologische Deutung. Geol. Bavarica **67**, 11–34, 1973

Breemen, van O., Aftalion, M., Bowes, D.R., Dudek, A., Misat, Z., Povondra, P., Vrána, S.: Geochronological studies of the Bohemian massif, Czechoslovakia, and their significance in the evolution of Central Europe. Trans. R. Soc. Edin.: Earth Sciences **73**, 89–108, 1982

Brown, R.L., Journeay, J.M., Lane, L.S., Murphy, D.C., Rees, C.J.: Obduction, backfolding and piggyback thrusting in the metamorphic hinterland of the southeastern Canadian Cordillera. J. Struct. Geol. **8**, 255–268, 1986

Christensen, N.I.: Compressional wave velocities in metamorphic rocks at pressures to 10 kbars. J. Geophys. Res. **70**, 6147–6164, 1965

DEKORP Research Group: First results and preliminary interpretation of deep-reflection seismic recordings along profile DEKORP 2-South. J. Geophys. **57**, 137–163, 1985

Edel, J.B.: Le socle Varisque de l'Europe moyenne apports du magnétisme et de la gravimétrie. Sci. Geol. Bull. **35**, 207–224, 1982

Edel, J.B., Coulon, M., Hernot, M.-P.: Mise en évidence par le paléomagnétisme d'une importante rotation antihoraire des Vosges méridionales entre le Viséen terminal et le Westphalien supérieur. Tectonophysics **106**, 239–257, 1984

Eisbacher, G., Krohe, A.: Kontinentales Tiefbohrprogramm der Bundesrepublik Deutschland. Ergebnisse der Vorerkundungsarbeiten Lokation Schwarzwald. 2. KTB Kolloquium, Seeheim/Odenwald 19–21 September, 1986, 1986

Emmert, U.: Perm nördlich der Alpen. In: Erläuterungen zur Geologischen Karte von Bayern 1:500000, 3. Auflage, Haunschild, H., Jerz, H., eds.: pp. 5–29, München, 1981

Franke, W.: Variszischer Deckenbau im Raume der Münchberger Gneismasse – abgeleitet aus der Fazies, Deformation und Metamorphose im umgebenden Paläozoikum. Geotekt. Forsch. **68**, 1–153, 1984a

Franke, W.: Late events in the tectonic history of the Saxothuringian zone. In: Variscan tectonics of the North Atlantic region: Hutton, D.W.H., Sanderson, D.J., eds.: pp. 33–45. Blackwell Scientific Publications, 1984b

Franke, W.: Development of the Central European Variscides – a review. In: Proceedings 3rd Workshop on the European Geotraverse (EGT) Project, Freeman, R., Müller, St., Giese, P., eds.: pp. 65–72. European Science Foundation 1986

Fuchs, H.K., Soffel, H.: Untersuchungen am Westabbruch der Böhmischen Einheit im oberfränkisch-oberpfälzischen Bruchschollenland mit Hilfe der Gravimetrie. N. Jb. Geol. Paläont. Mh. **1981**, 193–210, 1981

Grauert, B., Wänny, R., Soptrajanova, G.: Geochronology of a polymetamorphic and anatectic gneiss region: the Moldanubicum of the Area Lam – Deggendorf, Eastern Bavaria, Germany. Contr. Mineral. Petrol. **45**, 37–63, 1974

Gudden, H., Schmid, W.: Die Forschungsbohrung Obernsees. Geol. Bavarica **88**, 5–21, München, 1985

Haak, V., Blümecke, T.: In: Excursion guide Oberpfalz, Weber, K.: 2nd Int. Symposium on observation of the continental crust through drilling. Seeheim/ Odenwald 7–9 October, 1985, 1985

Haunschild, W., Schröder, B.: Geologische Karte von Bayern 1:25000, Blatt 6237, Grafenwöhr mit Erläuterungen. Bayer. Geol. Landesamt, München, 1960

Helmkampf, K.E., Kuhlmann, J., Kaiser, D.: Das Rotliegende im Randbereich der Weidener Bucht. Geol. Bavarica **83**, 167–186, München, 1982

Horn, P., Köhler, H., Müller-Sohnius, D.: A Rb/Sr WR-isochron ("fluid inclusion") age of the Bayerischer Pfahl, eastern Bavaria. Terra Cognita **3**, 199, 1983

Kern, H., Schenk, V.: Elastic wave velocities in rocks from the lower crustal section in southern Calabria (Italy). Phys. Earth Planet. Inter. **40**, 147–160, 1985

Kim, I.-S., Soffel, H.C.: Palaeomagnetic results of Lower Palaeozoic diabases and pillow lavas from the Frankenwald area (northwestern edge of the Bohemian Massif). J. Geophys. **51**, 24–28, 1982

Köhler, H., Müller-Sohnius, D.: Ergänzende Rb-Sr Altersbestimmung an Mineral- und Gesamtgesteinsproben des Leuchtenberger und des Flossenbürger Granits (NE Bayern). N. Jb. Miner., Mh. 1976, **8**, 354–365, 1976

Kossmat, F.: Gliederung des variszischen Gebirgsbaues. Abh. sächs. Geol. Landesamt **1**, 39 p., 1927

Krs, M.: Palaeomagnetic evidence of tectonic deformation of blocks in the Bohemian Massif. Geology **31**, 141–150, 1978

KTB 1986: Kontinentales Tiefbohrprogramm der Bundesrepublik Deutschland, KTB, Ergebnisse der Vorerkundungsarbeiten Lokation Oberpfalz, Weber, K. and Vollbrecht, A., eds.: 2. KTB-Kolloquium Seeheim/Odenwald, 19–21 September 1986, 1986

Leitz, F., Schröder, B.: Die Randfazies der Trias und das Bruchschollenland südöstlich Bayreuth (Exkursion C). Jber. Mitt. Oberrhein. Geol. Ver., N.F. **67**, 51–63, Stuttgart, 1985

Lenz, H.: Rb/Sr Gesamtgestein-Altersbestimmung am Weißenstadt-Marktleuthener Porphyrgranit des Fichtelgebirges. Geol. Jb. **E34**, 67–76, 1986

Lüschen, E. et al.: Near-vertical and wide-angle seismic surveys in the Black Forest, SW Germany. J. Geophys. **62**, 1–30, 1987

Matte, P.: La chaîne Varisque parmi les chaînes paléozoïques périatlantiques, modèle d'évolution et position des grands blocs continentaux au Permo-Carbonifère. Bull. Soc. Géol. France **8**, (II), 9–24, 1986a

Matte, P.: Tectonics and plate tectonics model for the Variscan Belt of Europe. Tectonophysics **126**, 329–374, 1986b

Matthews, D.H., Cheadle, M.J.: Deep reflection from the Caledonides and Variscides west of Britain. In: Reflection seismology: a global perspective, Barazangi, M., Brown, L., eds.: pp. 5–19. Geodynamics Series **13**, 1986

Matthews, D.H. and the BIRPS group: Some unsolved BIRPS problems. Geophys. J.R. Astron. Soc. **89**, 209–216, 1987

McGeary, S.: Nontypical BIRPS on the margin of the North Sea: The SHET Survey. Geophys. J.R. Astron. Soc. **89**, 231–238, 1987

Meissner, R., Bartelsen, H., Krey, Th., Schmoll, J.: Detecting velocity anomalies in the region of the Urach geothermal anomaly by means of new seismic field arrangements. In: Geothermics and geothermal energy, Cermak, V., Haenel, R., eds.: pp. 285–292, Stuttgart: E. Schweizerbart'sche Verlagsbuchhandlung, 1982

Mielke, H. et al.: Regional low-pressure metamorphism of low and medium grade in metapelites and -psammites of the Fichtelgebirge area, NE Bavaria. N. Jb. Miner. Abh. **137**, 83–112, 1979

Oxburgh, E.R.: Flake tectonics and continental collision. Nature **239**, 202–204, 1972

Perroud, H.: Contribution a l'étude paléomagnétique de l'arc ibéro-armoricain. Bull. Soc. Géol. Minéral. Bretagne **15**, 1–114, 1982

Price, R.A.: The southeastern Canadian Cordillera: thrust faulting, tectonic wedging, and delamination of the lithosphere. J. Struct. Geol. **8**, 239–254, 1986

Richter, P., Stettner, G.: Geochemische und petrographische Untersuchungen der Fichtelgebirgsgranite. Geol. Bavarica **78**, 144 p., 1979

Ries, A.C., Richardson, A., Shakleton, R.P.: Rotation of the Iberian arc; paleomagnetic results from North Spain. Earth Planet. Sci. Lett. **50**, 301–310, 1980

Royer, J.Y.: Etude paléomagnétique et géochronologique de Vosges cristallines du Nord. Mem. DEA, Institut Physique du Globe, Strasbourg I, 1982

Sandmeier, K.-J., Wenzel, F.: Synthetic seismograms for a complex crustal model. Geophys. Res. Lett. **13**, 22–25, 1986

Schreyer, W.: Metamorpher Übergang Moldanubikum/Saxothuringikum östlich Tirschenreuth/Opf., nachgewiesen durch phasenpetrologische Analyse. Geol. Rdsch. **55**, 491–509, 1966

Schröder, B., Siegling, M.: Geologische Karte von Bayern 1:25000, Blatt 6137, Kemnath mit Erläuterungen. Bayer. Geol. Landesamt, München, 1966

Schüssler, U., Oppermann, U., Kreuzer, H., Seidel, E., Okrusch, M., Lenz, K.-L., Raschka, H.: Zur Altersstellung des ostbayerischen Kristallins. Ergebnisse neuer K-Ar-Datierungen. Geol. Bavarica **89**, 21–47, 1986

Stein, E.: Die strukturgeologische Entwicklung im Übergangsbereich Saxothuringikum/Moldanubikum in NE-Bayern. Diss. Universität Göttingen, 125 p., 1987

Stettner, G.: Zur geotektonischen Entwicklung im Westteil der Böhmischen Masse bei Berücksichtigung des Deformationsstils im orogenen Bewegungssystem. Z.Dt. Geol. Ges. **123**, 291–326, 1972

Stettner, G.: Der Grenzbereich Saxothuringikum-Moldanubische Region im Raum Tirschenreuth-Mähring (Oberpfalz) und die Situation des Uran-führenden Präkambriums. Z.Dt. Geol. Ges. **130**, 561–574, 1979

Stettner, G.: Grundgebirge. In: Erläuterungen zur Geologischen Karte von Bayern 1:500000, 3. Auflage, Haunschild, H., Jerz, H., eds.: pp. 5–29, München, 1981

Strössenreuther, U.: Die Struktur der Erdkruste am Südwestrand der Böhmischen Masse, abgeleitet aus refraktions-seismischen Messungen der Jahre 1970 und 1978/79. Diss. Ludwig-Maximilians Universität, München, 1982

Taner, M.T., Koehler, F., Alhilali, K.A.: Estimation and correction of near-surface time anomalies (CDP static correction). Geophysics **39**, 441–463, 1974

Tapponier, P., Molnar, P.: Slip-line field theory and large-scale continental tectonics. Nature **264**, 319–324, 1976

Teufel, S.: Vergleichende U-Pb- und Rb-Sr-Altersbestimmungen an Gesteinen des Übergangsbereiches Saxothuringikum/Moldanubikum, NE-Bayern. Diss. Universität Göttingen, 110 p., 1987

Tollmann, A.: Großräumiger variszischer Deckenbau im Moldanubikum und neue Gedanken zum Variszikum Europas. Geotekt. Forsch. **64**. Stuttgart: Schweizerbart'sche Verlagsbuchhandlung, 1982

Wagener-Lohse, C., Blümel, P.: Prograde Niederdruckmetamorphose und ältere Mitteldruckmetamorphose im Nordostbayerischen Abschnitt der Grenzzone Saxothuringikum/Moldanubikum (Abstract): Jahrestagg. Geol. Ver., Gießen 1986, p. 84, 1986

de Wall, H.: Mikrostrukturelle Untersuchungen und strukturgeologische Kartierung der Gesteine aus dem Übergangsbereich Moldanubikum/Saxothuringikum westl. Mähring, Oberpfalz. Dipl.-Arb., Universität Göttingen, 1987

Weber, K.: The Mid-European Variscides in terms of allochthonous terraines. In: Proceedings of the 3rd EGT workshop, Bad Honnef, Freeman, R., Mueller, St., Giese, P., eds.: pp. 73–81. European Science Foundation 1986

Weber, K., Behr, H.J.: Geodynamic interpretation of the mid-European Variscides. In: Intracontinental fold belts – case studies in the Variscan Belt of Europe and the Damara Belt in Namibia, Martin, H., Eder, W., eds.: pp. 427–469. Springer Verlag, 1983

Ziegler, P.A.: Caledonian and Hercynian crustal consolidation of Western and Central Europe – a working hypothesis. Geol. en Mijnbouw **63**, 93–108, 1984

Zoubek, V.: Korrelation des präkambrischen Sockels der Mittel- und Westeuropäischen Varisziden. Z. Geol. Wiss. **7**, 1057–1064, 1979

Received August 6, 1987; revised version October 19, 1987
Accepted October 21, 1987